Molecular Pharmacology Fast Forward. Published on January 26, 2023 as DOI: 10.1124/molpharm.122.000618
This article has not been copyedited and formatted. The final version may differ from this version.

Genetic Knockout of Fatty Acid Amide Hydrolase (FAAH) Ameliorates Cisplatin-induced Nephropathy in Mice

Chaoling Chen [1], Weili Wang [1], Marissa Raymond [1], Fereshteh Ahmadinejad, Justin L. Poklis [1], Brandon Em [1], David A. Gewirtz [1], Aron H. Lichtman [1], Ningjun Li [1]

[1] Department of Pharmacology & Toxicology, Medical College of Virginia Campus, Virginia Commonwealth University, Richmond, VA 23298, USA

Downloaded from molpharm.aspetjournals.org at ASPET Journals on April 19, 2024

Molecular Pharmacology Fast Forward. Published on January 26, 2023 as DOI: 10.1124/molpharm.122.000618
This article has not been copyedited and formatted. The final version may differ from this version.

Running title page:

Fatty acid amide hydrolase in cisplatin nephrotoxicity

Correspondence to:

Dr. Ningjun Li

Department of Pharmacology & Toxicology,

Medical College of Virginia Campus,

Virginia Commonwealth University,

P.O. Box 980613

Richmond, VA 23298, USA

Tel: +1-804-828-2071

Fax: +1-804-828-4794

E-mail: nli@vcu.edu

Number of text pages: 40

Number of tables: 0

Number of figures: 9

Number of references: 69

Number of words in abstract: 250

Number of words in introduction: 390

Downloaded from molpharm.aspetjournals.org at ASPET Journals on April 19, 2024

Molecular Pharmacology Fast Forward. Published on January 26, 2023 as DOI: 10.1124/molpharm.122.000618
This article has not been copyedited and formatted. The final version may differ from this version.

Number of words in discussion: 1239

Abbreviations :

AEA, anandamide; AKI, acute kidney injury; 2-AG, 2-arachidonoylglycerol; BUN, blood urea nitrogen; CB, cannabinoids receptors; Cis, cisplatin; CKD, chronic kidney disease; FAAH, fatty acid amide hydrolase; HNSCC, head and neck squamous cell carcinoma; KIM-1, kidney injury molecule-1; NF-κB, nuclear factor-κB; OEA, oleoylethanolamide; PEA, palmitoylethanolamide; PF, PF-04457845

Downloaded from molpharm.aspetjournals.org at ASPET Journals on April 19, 2024

Molecular Pharmacology Fast Forward. Published on January 26, 2023 as DOI: 10.1124/molpharm.122.000618
This article has not been copyedited and formatted. The final version may differ from this version.

Abstract

Cisplatin is a potent first-line therapy for many solid malignancies such as breast, ovarian, lung, testicular and head and neck cancer. However, acute kidney injury (AKI) is a major dose-limiting toxicity in cisplatin therapy, which often hampers the continuation of cisplatin treatment. The endocannabinoid system, consisting of anandamide (AEA) and 2-arachidonoylglycerol and cannabinoid receptors, participates in different kidney diseases. Inhibition of fatty acid amide hydrolase (FAAH), the primary enzyme for the degradation of AEA and AEA-related N-acylethanolamines, elicits anti-inflammatory effects; however, little is known about its role in cisplatin nephrotoxicity. The current study tested the hypothesis that genetic deletion of *Faah* mitigates cisplatin-induced AKI. Male wild-type C57BL6 (WT) and *Faah*$^{-/-}$ mice were administered a single dose of intraperitoneal injection of cisplatin (30 mg/kg) and euthanatized 72 hours later. *Faah*$^{-/-}$ mice showed a reduction of cisplatin-induced blood urea nitrogen, plasma creatinine levels, kidney injury markers and tubular damage in comparison with WT mice. The renal protection from *Faah* deletion was associated with enhanced tone of AEA-related N-acylethanolamines (PEA and OEA), attenuated NF-κB/p65 activity, DNA damage markers p53, p21 and decreased expression of the inflammatory cytokine IL-1β as well as infiltration of macrophages and leukocytes in the kidneys. Notably, a selective FAAH inhibitor (PF-04457845) did not interfere with or perturb the antitumor effects of cisplatin in two head and neck squamous cell carcinoma cell lines, HN30 and HN12. Our work highlights that FAAH inactivation prevents cisplatin-induced nephrotoxicity in mice and that targeting FAAH could provide a novel strategy to mitigate cisplatin-induced nephrotoxicity.

Downloaded from molpharm.aspetjournals.org at ASPET Journals on April 19, 2024

Molecular Pharmacology Fast Forward. Published on January 26, 2023 as DOI: 10.1124/molpharm.122.000618
This article has not been copyedited and formatted. The final version may differ from this version.

Significance Statement

Mice lacking the *Faah* gene are protected from cisplatin-induced inflammation, DNA damage response, tubular damages and kidney dysfunction. Inactivation of FAAH could be a potential strategy to mitigate cisplatin-induced nephrotoxicity.

Downloaded from molpharm.aspetjournals.org at ASPET Journals on April 19, 2024

Molecular Pharmacology Fast Forward. Published on January 26, 2023 as DOI: 10.1124/molpharm.122.000618
This article has not been copyedited and formatted. The final version may differ from this version.

Introduction

Cisplatin is a potent first-line chemotherapy for many solid cancers. Acute kidney injury (AKI), a key factor contributing to the development of chronic kidney disease (CKD), represents a serious complication of cisplatin administration, which could disrupt the course of anticancer therapy. It is, therefore, critical to manage the cisplatin-induced AKI as early as possible in treatment. Exposure of renal cells to cisplatin results in damage to nuclear and mitochondria DNA, oxidative stress, activation of inflammation, and cellular senescence (Galluzzi et al., 2014). Ultimately, injured tubular cells lead to kidney dysfunction. Current approaches to management of cisplatin nephrotoxicity are very limited (Chen et al., 2022b).

The endocannabinoid system, consisting of cannabinoids receptors (CB1 and CB2) and their major ligands, N-arachidonoylethanolamine (anandamide; AEA) and 2-arachidonoylglycerol (2-AG), plays a role in different murine models of kidney disease (Moradi et al., 2016; Chen et al., 2022a). However, the role of fatty acid amide hydrolase (FAAH), the primary catalyzing enzyme of AEA, and other AEA-related N-acylethanolamides such as palmitoylethanolamide (PEA) and oleoylethanolamide (OEA), in cisplatin-induced AKI remains unspecified.

The Human Protein Atlas database and literature (Uhlen et al., 2015; Schlosser, 2017; Chen et al., 2022a) describe a high abundance of FAAH protein in the kidneys, suggesting that FAAH may play a role in renal modulation. Interestingly, mice with FAAH inhibitor treatment or genetic deletion of FAAH show protection from inflammation, hypertension and renal fibrogenesis (Ahn et al., 2009; Ahmad et al., 2018; Chen et al.,

Downloaded from molpharm.aspetjournals.org at ASPET Journals on April 19, 2024

Molecular Pharmacology Fast Forward. Published on January 26, 2023 as DOI: 10.1124/molpharm.122.000618
This article has not been copyedited and formatted. The final version may differ from this version.

2022a). Specifically, FAAH inactivation leads to reduced proinflammatory factors such as IL-1β, oxidative/nitrative stress and apoptosis (Bátkai et al., 2007; Greco et al., 2020; Chen et al., 2022a). Additionally, a growing body of research shows that FAAH blockade or an injection of FAAH substrates reduces NF-κB activation (Bátkai et al., 2007; Di Paola et al., 2012; Sayd et al., 2015; Genovese et al., 2022). In particular, we recently also reported that deletion of the *Faah* gene attenuated kidney damage in a mouse model of post ischemia/reperfusion renal fibrosis (Chen et al., 2022a).This study also demonstrated that both pharmacological and genetic inactivation of FAAH inhibited transforming growth factor-β1 (TGF-β1) -induced proinflammatory and profibrotic effects, indicative of the beneficial role of FAAH inhibition in the kidneys. Therefore, the purpose of this study was to test whether FAAH blockade also provides protection in the cisplatin-induced AKI mouse model.

Downloaded from molpharm.aspetjournals.org at ASPET Journals on April 19, 2024

Molecular Pharmacology Fast Forward. Published on January 26, 2023 as DOI: 10.1124/molpharm.122.000618
This article has not been copyedited and formatted. The final version may differ from this version.

Materials and Methods

Animals

All animal studies have been carried out in accordance with the Guide for the Care and Use of Laboratory Animals as adopted and promulgated by the U.S. National Institutes of Health. The *Faah* (+/+) and (−/−) mice used in this study were littermates from a colony maintained in the Transgenic/Knock-Out Mouse Shared Resource at Virginia Commonwealth University on a C57BL/6 background. The colony was initially established from 129SvJ embryonic stem cell clones and intercrosses of 129SvJ-C57BL/6 FAAH+/− mice (Cravatt et al., 2001; Lichtman et al., 2002). Mice used in the current study backcrossed for more than 20 generations onto a C57BL/6J background. Four-month-old male littermate wild-type (WT, *Faah* $^{+/+}$) and *Faah* knockout (KO) mice (*Faah*$^{-/-}$). Mice were bred in the animal facility and housed in temperature-controlled (20−22°C) polycarbonate cages with corn cob bedding. Mice were housed 2-5 per cages in a 12:12 light/dark cycle and provided with standard rodent chow and water (Wise et al., 2009; Lyu et al., 2020). Housing, husbandry and experiments were approved by the Institutional Animal Care and Use Committee at Virginia Commonwealth University.

Mouse model of cisplatin-induced AKI

The cisplatin-induced acute kidney injury model was generated as described previously (Faubel et al., 2004; Li et al., 2020; Sears and Siskind, 2021). Mice (25 ± 5 g) were randomly divided into three groups: wild type + vehicle (WT-saline), wild type + Cisplatin (WT-Cis), and *Faah* KO + cisplatin (*Faah*$^{-/-}$ Cis). Cisplatin (cis-diamminedichloro-

Downloaded from molpharm.aspetjournals.org at ASPET Journals on April 19, 2024

Molecular Pharmacology Fast Forward. Published on January 26, 2023 as DOI: 10.1124/molpharm.122.000618
This article has not been copyedited and formatted. The final version may differ from this version.

platinum (II), Sigma-Aldrich, MO) was freshly prepared in sterile in 0.9% normal saline at a concentration of 1 mg/ml. To induce cisplatin nephrotoxicity, mice were treated with one dose of cisplatin (30 mg/kg, intraperitoneal injection). Control mice were given 0.9% normal saline (Mitazaki et al., 2011). Single high dose of cisplatin is the most commonly used model for studying cisplatin-induced AKI in rodents (Mitazaki et al., 2011; Zhang et al., 2014; Liu et al., 2018). This model results in sharp declines in renal function which mirrors patients with severe AKI. All mice were monitored daily for body weight loss until euthanasia 72 hrs post-cisplatin injection. Mice underwent deep isoflurane anesthesia for blood and renal tissue collection. Blood was collected via cardiac puncture. Fresh kidneys were flash frozen in liquid nitrogen or fixed in 4% paraformaldehyde.

Renal function analysis

Renal function was determined by the levels of plasma creatinine and BUN by using LabAssay Creatinine kit (Fujifilm, Japan) and Vet Axcel Chemistry Analyzer (Alfa Wassermann, NJ) with Urea Nitrogen Reagent Kit, respectively (Xie et al., 2021; Chen et al., 2022a).

Western blot

Western blot analysis was performed as previously described (Hu et al., 2021; Chen et al., 2022a). Mouse renal cortex was homogenized in Tris-lysis buffer containing protease and phosphatase inhibitors (Sigmafast™ Protease Inhibitor Cocktail Tablet, Sigma Aldrich, MO) followed by sonication, centrifuge and boiled at 100°C for 10 minutes in 4X protein loading buffer. Total protein (15μg) was loaded into 12% polyacrylamide gel and then transferred onto a PVDF membrane by electroblotting.

Downloaded from molpharm.aspetjournals.org at ASPET Journals on April 19, 2024

Molecular Pharmacology Fast Forward. Published on January 26, 2023 as DOI: 10.1124/molpharm.122.000618
This article has not been copyedited and formatted. The final version may differ from this version.

Membranes were blocked with 5% nonfat dry milk (BioRad Laboratories, CA) in Tris-buffered saline with 0.1% Tween® 20 detergent and incubated with rabbit primary antibodies against kidney injury molecule-1 (KIM-1, PA1-86790, Cell Signaling Technology, MA), cleaved caspase-1 (NBP1-45433, Novus biologicals, CO) or mouse primary antibodies against IL-1β (12242, Cell Signaling Technology, MA), p53 (OP03T-10UG, Oncogene, CA) or p21 (sc-6246, Santa Cruz, CA) in a dilution of 1:1000 overnight at 4°C. GAPDH (60004-1-Ig, 1:5000, Proteintech, IL) was used as internal control. Blot signals were amplified by HRP-conjugated anti-rabbit or mouse secondary antibodies (Cell Signaling Technology, MA) in a concentration of 1:5000 for one hour and incubated with SuperSignal™ Western Blot Substrate Bundle (Thermo Fisher Scientific, MA). Protein bands were detected with Odyssey@ Fc imaging system and intensity of bands was determined using ImageJ software (NIH, http://rsbweb.nih.gov/ij/). All ratios of band intensities over GAPDH were obtained from each single sample and normalized to the mean value of the WT-saline group.

Immunohistochemical (IHC) staining in kidney tissues

Immunohistochemistry on paraffin-embedded kidney sections was performed as previously reported (Xie et al., 2021; Chen et al., 2022a). In brief, paraffin-embedded sections were deparaffinized and followed by subsequent antigen retrieval, endogenous peroxidase blocking with 3% H_2O_2, and nonspecific sites blocking in 10% serum. Rabbit primary antibodies against p65 (A19653, 1:100, ABclonal, MA), CD68 (250294, 1:300, ABBiotch Cruz, CA), CD43 (LS-C334703, 1:400, LSBio, WA) were incubated overnight at 4 °C. After incubating with rabbit secondary antibody for 1 hour at room temperature,

Downloaded from molpharm.aspetjournals.org at ASPET Journals on April 19, 2024

Molecular Pharmacology Fast Forward. Published on January 26, 2023 as DOI: 10.1124/molpharm.122.000618
This article has not been copyedited and formatted. The final version may differ from this version.

sections were proceeded to streptavidin HRP incubation, DAB staining, and counterstained with hematoxylin. At least 10 fields were obtained from high power microscope (400-fold magnification) for each sample (Yu et al., 2004; Yan and Ren, 2012). Positive cells were then calculated using ImageJ (NIH, http://rsbweb.nih.gov/ij/).

Histological examination by Periodic-Acid Schiff staining

Periodic-Acid Schiff staining (395B-1KT, Sigma Aldrich, MO) was utilized to assess histology of the kidneys. Kidney sections were incubated with periodic acid solution for 5 minutes and then placed in Schiff reagent for 15 minutes. Tubular damage is defined as tubular dilation, tubular atrophy, loss of brush border in proximal tubules, damage of tubular epithelial cells, vacuolization, and formation of tubular cast. The extent and scores of tubular injuries were determined on a scale of 0–4, as follows: 0 = no injury; 1 = 1–25% injured area; 2 = 26–50% injured area; 3 = 51–75% injured area; 4 > 75% injured area. Scoring of tubular injuries was semi-quantitatively assessed by two blinded evaluators blinded to treatment. At least 10 fields were obtained from a microscope (200-fold magnification) for the measurement of kidney tubular cast area by using ImageJ (Xie et al., 2021; Chen et al., 2022a).

Liquid chromatography-tandem mass spectrometry (LC-MS/MS) for measurement of lipids

The extraction and measurement of lipids were performed as we previously reported (Ritter et al., 2012; Chen et al., 2022a). AEA, 2AG, arachidonic acid (AA), PEA and OEA of mouse kidney cortex were measured by the Sciex 6500+ LC-MS/MS. The

Downloaded from molpharm.aspetjournals.org at ASPET Journals on April 19, 2024

Molecular Pharmacology Fast Forward. Published on January 26, 2023 as DOI: 10.1124/molpharm.122.000618
This article has not been copyedited and formatted. The final version may differ from this version.

weighed tissues were homogenized in 2 ml of chloroform/methanol (2:1 v/v containing 2 pmol AEA-d_8, 5 nmol 2-AG-d_8, 5 nmol AA-d_{11}, 0.625 nmol PEA-d_4 and OEA-d_4 as deuterated internal standards). Samples were added with 0.4ml of 0.73% sodium chloride mixture and vortexed for 2 mins. The organic phase was collected after centrifuged at 3000 rpm at 4°C for 5 minutes. The organic phases from the three extractions with 1ml of chloroform were pooled and dried under nitrogen gas. The dried residue was reconstituted in 0.1 ml of chloroform and mixed with 1 ml of cold acetone (Pharmco, Fisher Scientific, PA). After centrifugation for 10 min at 10000 rpm at 4°C, the upper layer was collected and dried under nitrogen gas. The extracts were reconstituted with 0.1 ml of methanol and transferred in an auto-sampler vials for analysis. The ultra-performance LC-MS/MS analysis was performed on a Sciex 6500 QTRAP system with an IonDrive Turbo V source for TurbolonSpray® (Sciex, Ontario, Canada) attached to a Shimadzu UPLC system (Kyoto, Japan) controlled by Analyst software (Sciex, Ontario, Canada). The following ion transitions (*m/z*) with collision energies (eV) in parentheses were monitored in positive ion mode: AEA: 348>62 (13) and 348>91 (60); AEA-d_8: 356 >63 (13); 2-AG: 379>287 (25) and 279 > 269 (29); 2-AG-d_8: 387>96 (25); PEA: 300>62 (28) and 300>283 (19); PEA-d_4: 304 > 62 (28); OEA: 326 > 62 (30) and 326 > 309 (20); OEA-d_4: 330 > 66 (30); and in negative mode: AA: 303 > 59 (-25) and 303 > 259 (-60); and AA-d_{11}: 314 > 59 (-60). Calibration curves were constructed for each assay based on peak area ratios for the calibrators and internal standards.

Cell culture and drug treatment

Downloaded from molpharm.aspetjournals.org at ASPET Journals on April 19, 2024

Molecular Pharmacology Fast Forward. Published on January 26, 2023 as DOI: 10.1124/molpharm.122.000618
This article has not been copyedited and formatted. The final version may differ from this version.

Two human papillomavirus-negative human head and neck squamous cell carcinoma (HNSCC) cell lines, HN30 (p53 wild-type) and HN12 (p53 mutant) were provided by Dr. Andrew Yeudall (Augusta University, GA). Cells were cultured in DMEM (Thermo Fisher Scientific, MA) supplemented with 10% (v/v) fetal bovine serum (GeminiBio, CA), 100 U/ml penicillin G sodium and 100 µg/ml streptomycin sulfate (Thermo Fisher Scientific, MA) at the 37°C incubator with 5% CO_2 (Ahmadinejad et al., 2022).

Downloaded from molpharm.aspetjournals.org at ASPET Journals on April 19, 2024

The inhibitory effects of FAAH inhibition and cisplatin in cancer cell lines by MTS assay

The sensitivity of HNSCC cell lines, HN30 (p53 wild-type) and HN12 (p53 mutant) to different doses of cisplatin, FAAH inhibitor (PF-04457845, Cayman Chemicals, MI) and the combination of the two drugs were tested by 3-(4,5-Dimethylthiazol-2-yl)-5-(3-carboxymethoxyphenyl)-2-(4-sulfophenyl)-2H-tetrazolium (Abcam, UK) MTS assay. Cancer cells were cultured in 96-well plates and pretreated with different concentrations of PF-04457845 (1 µM and 2 µM, Cayman, MI) 30 mins before cisplatin treatment (0 µM to 20 µM). On Day 3 and Day 6, 10% MTS was then added to the culture medium and incubated at 37°C for 4 hours. The absorbance was measured at the wavelengths 490 nm (Xie et al., 2022).

Toxicity of cisplatin and FAAH inhibition on cancer cells by clonogenic survival assay

Clonogenic survival assay was performed as previously described (Ahmadinejad et al., 2022; Xie et al., 2022). Cells were seeded at a low density (1 x 10^2 HN12 in 6-well

Molecular Pharmacology Fast Forward. Published on January 26, 2023 as DOI: 10.1124/molpharm.122.000618
This article has not been copyedited and formatted. The final version may differ from this version.

plates or 5 x 10^2 HN30 in 10 cm dishes), and exposed to 5 μM cisplatin in the absence and presence of 1 μM PF-04457845. Colony formation was observed over time, and at the experiment end point (when the vehicle-treated condition formed distinct colonies with more than 50 cells), colonies were fixed with 100% methanol, air-dried, and stained with 0.05% crystal violet and counted using a colony counter (COLOCOUNT Discovery Technology Intl, FL).

Statistical analysis

Data are presented as mean ± standard deviation (SD). GraphPad Prism 9.0 software was used for statistical analysis. The significance of differences in mean values between groups: WT-saline vs WT-cisplatin, WT-cisplatin vs *Faah* $^{-/-}$ cisplatin was evaluated using one-way ANOVA, followed by a Bonferroni's post hoc test (WT-saline vs. WT-Cis, WT-Cis vs. *Faah*$^{-/-}$Cis). $P < 0.05$ was considered statistically significant.

Results

1. **Genetic deletion of *Faah* improves cisplatin-induced renal dysfunction and kidney injury in mice.**

To investigate the role of *Faah* in cisplatin-induced kidney injury, we assessed renal function and kidney injury markers in WT and *Faah* $^{-/-}$ mice after cisplatin treatment. Cisplatin increased plasma creatinine (0.6 ± 0.2 mg/dL in WT-saline vs. 3.0 ± 0.9 mg/dL in WT-Cis , 95% CI : 1.2 to 3.7; $P = 0.0006$) and blood urea nitrogen (BUN) (23.8 ± 2.7 mg/dL in WT-saline vs. 156.6 ± 29.2 mg/dL in WT-Cis, 95% CI: 95.2 to 170.3; $P < 0.0001$) in WT mice (Figure 1A-B), whereas these effects were attenuated in *Faah* $^{-/-}$

Downloaded from molpharm.aspetjournals.org at ASPET Journals on April 19, 2024

Molecular Pharmacology Fast Forward. Published on January 26, 2023 as DOI: 10.1124/molpharm.122.000618
This article has not been copyedited and formatted. The final version may differ from this version.

mice (3.0 ± 0.9 vs. 1.4 ± 0.9 mg/dL in creatinine, 95% CI: 0.4 to 2.9; *P* = 0.0127 and 156.6 ± 29.2 vs. 81.8 ± 27.4 mg/dL in BUN, 95% CI: 37.27 to 112.3; *P* = 0.0005). Western blot analysis showed that cisplatin-induced upregulation of a kidney injury marker, kidney injury molecule-1 (KIM-1) in WT-cisplatin mice (increased by 3-fold, 95% CI: 1.9 to 4.4; *P* = 0.0005) was reduced in *Faah* $^{-/-}$ mice (WT-Cis vs. *Faah* $^{-/-}$ Cis: 3.1 vs.0.9 -fold, 95%: 1.1 to 3.3, *P* = 0.0004) (Figure 1C-D). These data suggest that genetic knockout of *Faah* may protect mice from cisplatin-induced renal dysfunction and kidney damage.

2. *Faah* deficiency reduces cisplatin-induced body weight loss, renal hypertrophy and tubular injuries.

We next examined the effects of cisplatin on the body weight and pathophysiological changes in the kidneys of *Faah*$^{-/-}$ mice. Cisplatin-induced body weight loss was reduced by approximately 20 % in *Faah*$^{-/-}$ mice (-19.5 vs. -14.3 % of body weight loss in WT-Cis vs. *Faah*$^{-/-}$ Cis, 95% CI: 2.8 to 7.7; *P* = 0.0003) (Figure 2A). Moreover, fresh kidneys following cisplatin treatment appeared larger and paler in WT mice than in *Faah*$^{-/-}$ mice (Figure 2B), suggesting that FAAH inactivation offers some protection from cisplatin-induced renal hypertrophy. Histological evaluation by Periodic-Acid Schiff (PAS) staining further showed that *Faah* deletion resulted in reductions of cisplatin-induced vacuolar degeneration, tubular atrophy, brush border loss and cast formation in tubules compared with WT group (3.6 vs. 2.4 points in WT-Cis vs. *Faah*$^{-/-}$ Cis, 95% CI: 0.8 to 1.6; *P* < 0.0001) (Figure 2C-D). Quantification of cast formation in kidneys revealed that *Faah* deletion decreased cast formation by about 50% in the presence of cisplatin

Downloaded from molpharm.aspetjournals.org at ASPET Journals on April 19, 2024

Molecular Pharmacology Fast Forward. Published on January 26, 2023 as DOI: 10.1124/molpharm.122.000618
This article has not been copyedited and formatted. The final version may differ from this version.

(13.18 ± 2.6 vs. 6.28 ± 1.4 % of cast area in WT-Cis vs. *Faah* $^{-/-}$ Cis, respectively, 95% CI: 4.1 to 9.7; $P < 0.0001$) (Figure 2E). These studies suggest that genetic deletion of *Faah* provides protection against cisplatin-associated body weight loss, kidney hypertrophy and tubular injuries.

3. Levels of two fatty acid ethanolamides, PEA and OEA but not endocannabinoids are increased in *Faah* KO cisplatin mice.

Furthermore, we questioned whether levels of substrates for FAAH including endocannabinoids (AEA and 2-AG) and other fatty acid ethanolamides PEA and OEA or the major metabolite of FAAH, arachidonic acid (AA) were changed in *Faah*$^{-/-}$ mice exposed to cisplatin. LC-MS/MS analysis demonstrated that there were no changes in AEA, 2-AG and AA between WT and *Faah*$^{-/-}$ mice after cisplatin treatment (WT-Cis vs. *Faah* $^{-/-}$ Cis: 0.2 vs. 0.3-fold in AEA, 95% CI: -0.3 to 0.6; $P > 0.99$, 0.9 vs. 0.8-fold in 2-AG, 95% CI: -0.4 to 0.2; $P = 0.84$, 0.8 vs. 0.5-fold in AA, 95% CI: -0.05 to 0.7, $P = 0.09$) (Figure 3A-C), suggesting that the renal protection against cisplatin in *Faah*$^{-/-}$ mice may not be related to the levels of AEA, 2-AG and AA. Instead, compared with renal cortex of WT cisplatin mice, *Faah*$^{-/-}$ Cis mice showed 1.45-fold increase of PEA levels (WT-Cis vs. *Faah* $^{-/-}$ Cis: 0.6 vs. 1-fold, 95% CI: 0.1 to 0.8; $P = 0.0109$) and 3-fold increase of OEA levels (0.9 vs. 2.9-fold, 95% CI: 1.5 to 2.5; $P < 0.0001$) (Figure 4A-D). These data indicated that the protection of *Faah*$^{-/-}$ mice against cisplatin-induced kidney injuries could be associated with enhanced PEA and OEA tone.

Downloaded from molpharm.aspetjournals.org at ASPET Journals on April 19, 2024

Molecular Pharmacology Fast Forward. Published on January 26, 2023 as DOI: 10.1124/molpharm.122.000618
This article has not been copyedited and formatted. The final version may differ from this version.

4. *Faah* knockout mice are protected from cisplatin-induced nuclear NF-κB/p65 translocation.

Nuclear factor-κB (NF-κB) p65 subunit is a key transcription factor that regulates inflammasome activation (Lawrence, 2009). Cisplatin is known to induce nuclear translocation of NF-κB p65 from the cytoplasm (Yeh et al., 2004; Xie et al., 2022), which is a critical step in producing many inflammatory cytokines as well as caspase-1-Interleukin (IL)-1β inflammasome activation (Lawrence, 2009; Lamkanfi and Dixit, 2014). We therefore tested the effect of *Faah* inhibition on cisplatin-induced NF-κB activation. Immunochemistry showed that cisplatin induced more nucleus translocation of the NF-κB subunit p65 in WT mice compared with saline-treated WT mice (increased approximately 45 positive cells/power field, 95% CI: 25.9 to 65.2; P = 0.0001). This cisplatin-induced activation/nucleus translocation was attenuated in *Faah*$^{-/-}$ cisplatin mice (decreased approximately 33 positive cells/power field compared with WT-Cis, 95% CI: 13.3 to 52.5; P = 0.0021) (Figure 5A-B). These results suggest that genetic knockout of *Faah* ameliorates cisplatin-induced activity and nuclear translocation of NF-κB subunit p65.

5. Cisplatin-induced activation of caspase-1 and interleukin-1β and infiltration of macrophages and leukocytes are ameliorated in *Faah* KO mice.

Caspase-1 activation promotes inflammatory cytokine interleukin-1 β (IL-1β) secretion; this process is predominantly regulated by NF-κB (Fujisawa et al., 2011; Mangali et al., 2019) and contributes to cisplatin-induced kidney injury (Aranda-Rivera et al., 2022). Western blot analysis demonstrated that cisplatin-induced activation of caspase-1

Downloaded from molpharm.aspetjournals.org at ASPET Journals on April 19, 2024

Molecular Pharmacology Fast Forward. Published on January 26, 2023 as DOI: 10.1124/molpharm.122.000618
This article has not been copyedited and formatted. The final version may differ from this version.

(cleaved form) was ~~markedly~~ increased in the renal cortex of WT mice (2.5-fold increase, 95% CI: 2.2 to 2.8; $P < 0.0001$), which was inhibited in *Faah*$^{-/-}$ mice (WT-Cis vs. *Faah*$^{-/-}$ Cis: 2.5 vs. 0.99 -fold increase, 95% CI: 0.34 to 1.6; $P < 0.0001$) (Figure 6A-B). Correspondingly, the increased generation of cleaved or activated form of IL-1β by cisplatin in WT mice was inhibited in *Faah*$^{-/-}$ mice as well (WT-Cis vs. *Faah*$^{-/-}$ Cis: 6.9 vs. 2.5-fold increase; 95% CI: 1.3 to 7.4; $P = 0.0067$) (Figure 6C-D).

Infiltration of macrophages and leukocytes is also a major mediator for cisplatin-induced nephrotoxicity (Sears and Siskind, 2021). Levels of inflammatory cell infiltration were determined by the expression of a macrophage marker, CD68 and a leukocyte marker, CD43 in the kidneys. Immunochemistry showed that cisplatin increased the expression of CD68 and CD43 in WT kidneys (Figure 6E, F, G), whereas deficiency of *Faah* gene reduced the upregulation of CD68 and CD43 in the kidneys (WT-Cis vs. *Faah*$^{-/-}$ Cis: 9.5 vs. 4.2-fold increase in CD68; $P = 0.0073$, 13.3 vs. 6.7 -fold increase in CD43; $P = 0.001$). Taken together, these results suggest that *Faah*$^{-/-}$ mice display attenuated renal inflammatory responses induced by cisplatin.

6. Cisplatin-induced DNA damage markers in the kidneys are decreased in *Faah-/-* mice.

Activation of p53/p21 pathway is an important indicator for cisplatin-induced DNA damage, which not only causes cell cycle arrest but also activates NF-κB and downstream proinflammatory factors (Mowla et al., 2013). Cell cycle arrest of tubular cells ultimately results in maladaptive repair of injured renal cells. Therefore, cisplatin-induced DNA damage response and the consequent tubular cell injury play early central

Downloaded from molpharm.aspetjournals.org at ASPET Journals on April 19, 2024

Molecular Pharmacology Fast Forward. Published on January 26, 2023 as DOI: 10.1124/molpharm.122.000618
This article has not been copyedited and formatted. The final version may differ from this version.

roles in the initial stage of AKI and the progression of kidney damage (Zhu et al., 2015). We therefore examined whether inactivation of FAAH would also interfere with the induction of DNA damage response in the kidneys. Western blot analysis showed that cisplatin treatment upregulated p53, which can activate the cell cycle inhibitor p21 in G2/M phase, in WT mouse kidneys (increased 6.5-fold, 95% CI: 1.1 to 12, P = 0.01) (Figure 7A-B). The cell cycle inhibitor p21 was also increased in WT-cisplatin mice (increased 22 -fold; 95% CI: 15.4 to 30.3; P <0.0001) (Figure 7C-D). On the other hand, *Faah*$^{-/-}$ mice showed a dampened cisplatin-induced upregulated expression of these proteins (WT-Cis vs. *Faah*$^{-/-}$ Cis: 6.4 vs. 2.4-fold in p53, 95% CI: 0.01 to 8.45; P = 0.049, 22 vs. 5.1-fold in p21; 95% CI: 11.8 to 23.5, P <0.0001) (Figure 7A-D). These data indicate that deletion of *Faah* also dampens cisplatin-induced DNA damage response in the kidneys.

6. Inhibition of FAAH does not interfere with the antitumor effects of cisplatin.

To evaluate whether inhibition of FAAH might perturb the anti-tumor effect of cisplatin, we tested the effect of pre-treatment of the FAAH inhibitor (PF-04457845, PF) on head and neck squamous cell carcinoma cell lines (HNSCC), HN30 (p53 wild-type) and HN12 (p53 mutant) followed by cisplatin treatment. The results from the MTS assay showed that different doses of the FAAH inhibitor did not diminish the effectiveness of cisplatin on HNSCC cell lines, HN12 and HN30 (Figure 8A-B), suggesting that inactivation of FAAH would not interfere with the antitumorigenic effects of cisplatin. Additionally, there was no difference in toxicity between the cisplatin alone group and Combo (cisplatin + PF) in these tumor cells by a clonogenic survival assay (Figure 8C-D). Overall, these

Downloaded from molpharm.aspetjournals.org at ASPET Journals on April 19, 2024

Molecular Pharmacology Fast Forward. Published on January 26, 2023 as DOI: 10.1124/molpharm.122.000618
This article has not been copyedited and formatted. The final version may differ from this version.

results suggest that inhibition of FAAH does not reduce or influence the anticancer effects of cisplatin.

Downloaded from molpharm.aspetjournals.org at ASPET Journals on April 19, 2024

Molecular Pharmacology Fast Forward. Published on January 26, 2023 as DOI: 10.1124/molpharm.122.000618
This article has not been copyedited and formatted. The final version may differ from this version.

Discussion

The current studies reveal that genetic deletion of *Faah*, the primary enzyme for the degradation of AEA and related fatty acid amides, alleviates cisplatin-induced AKI. This renal protection is associated with amelioration of renal kidney dysfunction, NF-κB activation, inflammatory factors and DNA damage responses in cisplatin nephrotoxicity. Hence, inactivation of FAAH could be a promising strategy for treating cisplatin-induced AKI.

Our current findings are consistent with literature showing the protective effects of FAAH inhibition in different kidney disease models and other organs (Bátkai et al., 2007; Chen et al., 2022a). *Faah* knockout mice were found to be protected from post ischemia reperfusion injury, inflammation and renal fibrogenesis in our previous report (Chen et al., 2022a). FAAH inhibition elicits diuretic and blood pressure-lowering effects in mice (Ahmad et al., 2018). In addition, a study showed that aging *Faah*$^{-/-}$ mice exhibited improved age-related cardiac dysfunction, and reduced myocardial nitrative stress and inflammation compared with wild-type littermates (Bátkai et al., 2007).

Inflammation and DNA damage response critically contribute to cisplatin nephrotoxicity (Ozkok and Edelstein, 2014; Zhu et al., 2015). It has been shown that an acute administration of cisplatin largely increases pro-inflammatory factors including caspase 1 and IL-1β (Ozkok et al., 2016). In addition, cisplatin plays a critical role in the induction of a DNA damage response, inhibition of injured renal tubular cells entering into G1/S cell cycle via the increased expression of p53 (Ryan et al., 2001) and the cyclin-dependent kinase inhibitor, p21CIP1/WAF1/SDI (Miyaji et al., 2001). Our results that genetic deletion of *Faah* attenuates the cisplatin-induced activation of NF-κB/p65

Downloaded from molpharm.aspetjournals.org at ASPET Journals on April 19, 2024

Molecular Pharmacology Fast Forward. Published on January 26, 2023 as DOI: 10.1124/molpharm.122.000618
This article has not been copyedited and formatted. The final version may differ from this version.

and the upregulation of inflammatory factors caspase-1, cleaved IL-1β (Figure 5-6) suggest that *Faah* inhibition may play roles in preventing cisplatin-induced nucleus translocation of NF-κB/p65 and inflammatory downstream effectors. Indeed, nuclear NF-κB/p65 translocation plays central roles in NLRP3/caspase-1 inflammasome activation, production of proinflammatory cytokines, and thereby a causal role in renal injury and DNA damage (Chien et al., 2011; Salminen et al., 2012; Hamad et al., 2015; Zhao and Wen, 2018). NLRP3/caspase-1 inflammasome activation has been suggested to induce pro-inflammatory cytokine IL-1β secretion which can trigger DNA damage (Yin et al., 2017; Romero et al., 2022). Previous studies have shown that IL-1β is able to induce the upregulation of DNA damage response markers p53/p21 (Dai et al., 2006; Yin et al., 2017; Shi et al., 2019). Subsequently, cells with DNA damage may become senescent and produce secretome which is enriched with chemokines, pro-inflammatory cytokines, growth factors (Rovillain et al., 2011; Salminen et al., 2012; Gorgoulis et al., 2019; Lopes-Paciencia et al., 2019; Shi et al., 2019). It is also shown that p53 and NF-κB co-regulate pro-inflammatory gene expression in macrophages (Lowe et al., 2014). Consistent with our findings, Jin et al (2019) reported that cisplatin treatment led to a induction of cellular senescence/ DNA damage response three days later (Jin et al., 2019). These findings are in agreement with the results from the present study demonstrating the protection of *Faah*$^{-/-}$ mice against cisplatin nephrotoxicity may involve in the attenuation of the positive feedback loop of increased p53/p21 DNA damage response pathway and the kidney inflammation (Sheekey and Narita, 2021).

FAAH is the primary catabolic enzyme for fatty acid amide family of endogenous lipids including anandamide (AEA), palmitoylethanolamide (PEA) and

Downloaded from molpharm.aspetjournals.org at ASPET Journals on April 19, 2024

Molecular Pharmacology Fast Forward. Published on January 26, 2023 as DOI: 10.1124/molpharm.122.000618
This article has not been copyedited and formatted. The final version may differ from this version.

oleoylethanolamide (OEA), and other lipid signaling molecules. Increased AEA levels in *Faah*$^{-/-}$ mice is associated with alleviation of renal inflammation after post ischemia reperfusion injury (Chen et al., 2022a). Interestingly, we found here that the renal protection from *Faah*$^{-/-}$ mice against cisplatin nephrotoxicity may be regulated by enhanced levels of AEA-related N-acylethanolamides (PEA and OEA) but not endocannabinoids AEA and 2-AG. In contrast to a previous study by Mukhopadhyay et al (Mukhopadhyay et al., 2010), we did not notice the increment of AEA in our WT-Cis mice. We speculated that the discrepancy would be due to susceptibility of different mouse strain to cisplatin treatment and the dose (25 mg/Kg vs. 30 mg/Kg). Furthermore, the decreased levels of AEA that were not recovered in *Faah*$^{-/-}$ Cis mice in our study may indicate the potential inhibitory effects of cisplatin on AEA-synthesizing enzyme.

Several reports have revealed that PEA and OEA possess anti-inflammatory effects and act as agonists for peroxisome proliferator-activated receptor alpha (PPAR-α) to inhibit NF-κB/p65 activation through cannabinoid receptors independent pathway (Lo Verme et al., 2005; Di Paola et al., 2012; Antón et al., 2017; Decara et al., 2020). It has been demonstrated that inhibition of NF-κB/p65 ameliorates cisplatin-induced AKI, pro-inflammatory mediators including caspase 1 and IL-1β (Ozkok et al., 2016). NF-κB pathway is known to activate many of the cytokines including interleukin-1, 4, 6, TNF-α, TGF-β1 and monocyte chemotactic protein-1 (MCP-1) (Peres and da Cunha, 2013). FAAH inhibition has been shown to reduce colitis-induced levels of proinflammatory factor such as IL-6, IL-1β, monocyte chemotactic protein-1 (MCP-1) as well as NF-κB (Winkler et al., 2016; Shamran et al., 2017; Genovese et al., 2022). We showed that NF-κB activation was inhibited in *Faah*$^{-/-}$Cis mice, suggesting FAAH inhibition may

Downloaded from molpharm.aspetjournals.org at ASPET Journals on April 19, 2024

Molecular Pharmacology Fast Forward. Published on January 26, 2023 as DOI: 10.1124/molpharm.122.000618
This article has not been copyedited and formatted. The final version may differ from this version.

reduce downstream cytokine productions. Shamran et al also demonstrated that FAAH inhibition reduces macrophage, neutrophil, NKT/NK and dendritic cell infiltration (Shamran et al., 2017), which is consistent with our finding that FAAH inhibition reduces infiltration of macrophages (CD68) and leukocytes (CD43). Consequently, we speculate that the mechanism of the protective actions of FAAH inactivation against cisplatin-induced AKI may be mediated by the enhancement of PEA ad OEA, which would inhibit the activation of NF-κB/p65 and the vicious cycle between DNA damage and inflammatory secretome. Further studies are needed to delineate the underlying mechanisms of the protective roles of endogenous fatty acid amides in cisplatin nephrotoxicity.

It is noteworthy that FAAH inhibition also provides protection against lung cancer cell metastasis and invasion, diffuse large B-cell lymphoma and in-vivo breast tumor growth (Winkler et al., 2016; Doan et al., 2018). Additionally, administration of a FAAH inhibitor mitigates cisplatin-induced vomiting in shrews (Parker et al., 2009) as well as hyper-nociception in mice (Uhelski et al., 2015). Furthermore, anticancer drugs-induced DNA damage response and consequent senescent cells are implicated to promote tumor growth and contribute to/exacerbate many adverse effects of chemotherapy (Demaria et al., 2017). It is possible that FAAH inhibition might also enhance the anti-tumor effects of cisplatin. However, we found that there was no interference of FAAH inhibition in cisplatin-treated head and neck cancer cells in our study (Figure 8). Thus, FAAH inhibition may provide a therapeutic strategy to prevent cisplatin toxicity without altering the effects of cisplatin.

Downloaded from molpharm.aspetjournals.org at ASPET Journals on April 19, 2024

Molecular Pharmacology Fast Forward. Published on January 26, 2023 as DOI: 10.1124/molpharm.122.000618
This article has not been copyedited and formatted. The final version may differ from this version.

It should be noted that the current study was performed in male mice. It is important to use female rodents as well in the current study. However, *in vivo* animal studies have shown a much higher sensitivity of cisplatin-induced kidney damage in males than in females (Eshraghi-Jazi et al., 2011) and that cisplatin produces >3 times increases of plasma creatinine and kidney KIM-1 levels in male mice than female mice (Boddu et al., 2017). To mix the male and female mice may complicate data interpretation. A separated study to investigate the renoprotective role of FAAH inhibition in females is required in future studies.

In summary, this study raises the possibility that inhibition of FAAH represents a viable strategy to mitigate cisplatin-induced nephrotoxicity, by reducing the activation of NF-κB/p65 and expression of DNA damage markers p53 and p21 as well as renal inflammation. The consequent reduction in the expression of inflammatory and DNA damage markers by FAAH inactivation ameliorates cisplatin nephrotoxicity (Figure 9).

Authorship Contributions

Participated in research design: Chen C, Raymond M, Ahmadinejad F, Gewirtz DA, Lichtman AH, Li N

Conducted experiments: Chen C, Wang W, Raymond M, Ahmadinejad F, Poklis JL, Em B.

Performed data analysis: Chen C, Raymond M, Ahmadinejad F, Poklis JL

Wrote or contributed to the writing of the manuscript: Chen C, Gewirtz DA, Li N. Lichtman AH

Downloaded from molpharm.aspetjournals.org at ASPET Journals on April 19, 2024

Molecular Pharmacology Fast Forward. Published on January 26, 2023 as DOI: 10.1124/molpharm.122.000618
This article has not been copyedited and formatted. The final version may differ from this version.

References

Ahmad A, Dempsey SK, Daneva Z, Li N, Poklis JL, Li PL and Ritter JK (2018) Modulation of mean arterial pressure and diuresis by renomedullary infusion of a selective inhibitor of fatty acid amide hydrolase. *Am J Physiol Renal Physiol* **315**:F967-F976.

Ahmadinejad F, Bos T, Hu B, Britt E, Koblinski J, Souers AJ, Leverson JD, Faber AC, Gewirtz DA and Harada H (2022) Senolytic-Mediated Elimination of Head and Neck Tumor Cells Induced Into Senescence by Cisplatin. *Mol Pharmacol* **101**:168-180.

Ahn K, Johnson DS, Mileni M, Beidler D, Long JZ, McKinney MK, Weerapana E, Sadagopan N, Liimatta M, Smith SE, Lazerwith S, Stiff C, Kamtekar S, Bhattacharya K, Zhang Y, Swaney S, Van Becelaere K, Stevens RC and Cravatt BF (2009) Discovery and Characterization of a Highly Selective FAAH Inhibitor that Reduces Inflammatory Pain. *Chem Biol* **16**:411-420.

Antón M, Alén F, Gómez de Heras R, Serrano A, Pavón FJ, Leza JC, García-Bueno B, Rodríguez de Fonseca F and Orio L (2017) Oleoylethanolamide prevents neuroimmune HMGB1/TLR4/NF-kB danger signaling in rat frontal cortex and depressive-like behavior induced by ethanol binge administration. *Addict Biol* **22**:724-741.

Aranda-Rivera AK, Srivastava A, Cruz-Gregorio A, Pedraza-Chaverri J, Mulay SR and Scholze A (2022) Involvement of Inflammasome Components in Kidney Disease. *Antioxidants* **11**:246.

Downloaded from molpharm.aspetjournals.org at ASPET Journals on April 19, 2024

Molecular Pharmacology Fast Forward. Published on January 26, 2023 as DOI: 10.1124/molpharm.122.000618
This article has not been copyedited and formatted. The final version may differ from this version.

Bátkai S, Rajesh M, Mukhopadhyay P, Haskó G, Liaudet L, Cravatt BF, Csiszár A, Ungvári Z and Pacher P (2007) Decreased age-related cardiac dysfunction, myocardial nitrative stress, inflammatory gene expression, and apoptosis in mice lacking fatty acid amide hydrolase. *Am J Physiol Heart Circ Physiol* **293**:H909-H918.

Boddu R, Fan C, Rangarajan S, Sunil B, Bolisetty S and Curtis LM (2017) Unique sex- and age-dependent effects in protective pathways in acute kidney injury. *Am J Physiol Renal Physiol* **313**:F740-f755.

Chen C, Wang W, Poklis JL, Lichtman AH, Ritter JK, Hu G, Xie D and Li N (2022a) Inactivation of fatty acid amide hydrolase protects against ischemic reperfusion injury-induced renal fibrogenesis. *Biochim Biophys Acta Mol Basis Dis* **1868**:166456.

Chen C, Xie D, Gewirtz DA and Li N (2022b) Nephrotoxicity in cancer treatment: An update. *Adv Cancer Res* **155**:77-129.

Chien Y, Scuoppo C, Wang X, Fang X, Balgley B, Bolden JE, Premsrirut P, Luo W, Chicas A, Lee CS, Kogan SC and Lowe SW (2011) Control of the senescence-associated secretory phenotype by NF-κB promotes senescence and enhances chemosensitivity. *Genes Dev* **25**:2125-2136.

Cravatt BF, Demarest K, Patricelli MP, Bracey MH, Giang DK, Martin BR and Lichtman AH (2001) Supersensitivity to anandamide and enhanced endogenous cannabinoid signaling in mice lacking fatty acid amide hydrolase. *Proc Natl Acad Sci U S A* **98**:9371-9376.

Downloaded from molpharm.aspetjournals.org at ASPET Journals on April 19, 2024

Molecular Pharmacology Fast Forward. Published on January 26, 2023 as DOI: 10.1124/molpharm.122.000618
This article has not been copyedited and formatted. The final version may differ from this version.

Dai SM, Shan ZZ, Nakamura H, Masuko-Hongo K, Kato T, Nishioka K and Yudoh K (2006) Catabolic stress induces features of chondrocyte senescence through overexpression of caveolin 1: possible involvement of caveolin 1-induced down-regulation of articular chondrocytes in the pathogenesis of osteoarthritis. *Arthritis Rheum* **54**:818-831.

Decara J, Rivera P, López-Gambero AJ, Serrano A, Pavón FJ, Baixeras E, Rodríguez de Fonseca F and Suárez J (2020) Peroxisome Proliferator-Activated Receptors: Experimental Targeting for the Treatment of Inflammatory Bowel Diseases. *Front Pharmacol* **11**:730.

Demaria M, O'Leary MN, Chang J, Shao L, Liu S, Alimirah F, Koenig K, Le C, Mitin N, Deal AM, Alston S, Academia EC, Kilmarx S, Valdovinos A, Wang B, de Bruin A, Kennedy BK, Melov S, Zhou D, Sharpless NE, Muss H and Campisi J (2017) Cellular Senescence Promotes Adverse Effects of Chemotherapy and Cancer Relapse. *Cancer Discov* **7**:165-176.

Di Paola R, Impellizzeri D, Mondello P, Velardi E, Aloisi C, Cappellani A, Esposito E and Cuzzocrea S (2012) Palmitoylethanolamide reduces early renal dysfunction and injury caused by experimental ischemia and reperfusion in mice. *Shock* **38**:356-366.

Doan T, Sun J, Henderson J, Du Y and Mohan C (2018) Targeting FAAH in hematological and non-hematological cancers. *The Journal of Immunology* **200**:178.120-178.120.

Eshraghi-Jazi F, Nematbakhsh M, Nasri H, Talebi A, Haghighi M, Pezeshki Z, Safari T and Ashrafi F (2011) The protective role of endogenous nitric oxide donor (L-

Downloaded from molpharm.aspetjournals.org at ASPET Journals on April 19, 2024

Molecular Pharmacology Fast Forward. Published on January 26, 2023 as DOI: 10.1124/molpharm.122.000618
This article has not been copyedited and formatted. The final version may differ from this version.

arginine) in cisplatin-induced nephrotoxicity: Gender related differences in rat model. *J Res Med Sci* **16**:1389-1396.

Faubel S, Ljubanovic D, Reznikov L, Somerset H, Dinarello CA and Edelstein CL (2004) Caspase-1-deficient mice are protected against cisplatin-induced apoptosis and acute tubular necrosis. *Kidney Int* **66**:2202-2213.

Fujisawa T, Chang MM, Velichko S, Thai P, Hung LY, Huang F, Phuong N, Chen Y and Wu R (2011) NF-κB mediates IL-1β- and IL-17A-induced MUC5B expression in airway epithelial cells. *Am J Respir Cell Mol Biol* **45**:246-252.

Galluzzi L, Vitale I, Michels J, Brenner C, Szabadkai G, Harel-Bellan A, Castedo M and Kroemer G (2014) Systems biology of cisplatin resistance: past, present and future. *Cell Death Dis* **5**:e1257.

Genovese T, Duranti A, D'Amico R, Fusco R, Impellizzeri D, Peritore AF, Crupi R, Gugliandolo E, Cuzzocrea S, Di Paola R, Siracusa R and Cordaro M (2022) Fatty Acid Amide Hydrolase (FAAH) Inhibition Plays a Key Role in Counteracting Acute Lung Injury. *Int J Mol Sci* **23**:2781.

Gorgoulis V, Adams PD, Alimonti A, Bennett DC, Bischof O, Bishop C, Campisi J, Collado M, Evangelou K, Ferbeyre G, Gil J, Hara E, Krizhanovsky V, Jurk D, Maier AB, Narita M, Niedernhofer L, Passos JF, Robbins PD, Schmitt CA, Sedivy J, Vougas K, von Zglinicki T, Zhou D, Serrano M and Demaria M (2019) Cellular Senescence: Defining a Path Forward. *Cell* **179**:813-827.

Greco R, Demartini C, Zanaboni AM, Tumelero E, Reggiani A, Misto A, Piomelli D and Tassorelli C (2020) FAAH inhibition as a preventive treatment for migraine: A pre-clinical study. *Neurobiol Dis* **134**:104624.

Downloaded from molpharm.aspetjournals.org at ASPET Journals on April 19, 2024

Molecular Pharmacology Fast Forward. Published on January 26, 2023 as DOI: 10.1124/molpharm.122.000618
This article has not been copyedited and formatted. The final version may differ from this version.

Hamad R, Jayakumar C, Ranganathan P, Mohamed R, El-Hamamy MM, Dessouki AA, Ibrahim A and Ramesh G (2015) Honey feeding protects kidney against cisplatin nephrotoxicity through suppression of inflammation. *Clin Exp Pharmacol Physiol* **42**:843-848.

Hu G, Zhu Q, Wang W, Xie D, Chen C, Li PL, Ritter JK and Li N (2021) Collecting duct-specific knockout of sphingosine-1-phosphate receptor 1 aggravates DOCA-salt hypertension in mice. *J Hypertens* **39**:1559-1566.

Jin H, Zhang Y, Ding Q, Wang SS, Rastogi P, Dai D-F, Lu D, Purvis M, Cao C, Wang A, Liu D, Ren C, Elhadi S, Hu M-C, Chai Y, Zepeda-Orozco D, Campisi J and Attanasio M (2019) Epithelial innate immunity mediates tubular cell senescence after kidney injury. *JCI Insight* **4**:e125490.

Lamkanfi M and Dixit VM (2014) Mechanisms and functions of inflammasomes. *Cell* **157**:1013-1022.

Lawrence T (2009) The nuclear factor NF-kappaB pathway in inflammation. *Cold Spring Harb Perspect Biol* **1**:a001651.

Li F, Sun A, Cheng G, Liu D, Xiao J, Zhao Z and Dong Z (2020) Compound C Protects Against Cisplatin-Induced Nephrotoxicity Through Pleiotropic Effects. *Front Physiol* **11**:614244.

Lichtman AH, Hawkins EG, Griffin G and Cravatt BF (2002) Pharmacological Activity of Fatty Acid Amides Is Regulated, but Not Mediated, by Fatty Acid Amide Hydrolase in Vivo. *J Pharmacol Exp Ther* **302**:73-79.

Downloaded from molpharm.aspetjournals.org at ASPET Journals on April 19, 2024

Molecular Pharmacology Fast Forward. Published on January 26, 2023 as DOI: 10.1124/molpharm.122.000618
This article has not been copyedited and formatted. The final version may differ from this version.

Liu J, Livingston MJ, Dong G, Tang C, Su Y, Wu G, Yin X-M and Dong Z (2018) Histone deacetylase inhibitors protect against cisplatin-induced acute kidney injury by activating autophagy in proximal tubular cells. *Cell Death Dis* **9**:322.

Lo Verme J, Fu J, Astarita G, La Rana G, Russo R, Calignano A and Piomelli D (2005) The nuclear receptor peroxisome proliferator-activated receptor-alpha mediates the anti-inflammatory actions of palmitoylethanolamide. *Mol Pharmacol* **67**:15-19.

Lopes-Paciencia S, Saint-Germain E, Rowell M-C, Ruiz AF, Kalegari P and Ferbeyre G (2019) The senescence-associated secretory phenotype and its regulation. *Cytokine* **117**:15-22.

Lowe JM, Menendez D, Bushel PR, Shatz M, Kirk EL, Troester MA, Garantziotis S, Fessler MB and Resnick MA (2014) p53 and NF-κB coregulate proinflammatory gene responses in human macrophages. *Cancer Res* **74**:2182-2192.

Lyu B, Wang W, Ji X-Y, Ritter JK and Li N (2020) Detrimental role of sphingosine kinase 1 in kidney damage in DOCA-salt hypertensive model: evidence from knockout mice. *BMC Nephrology* **21**:173.

Mangali S, Bhat A, Udumula MP, Dhar I, Sriram D and Dhar A (2019) Inhibition of protein kinase R protects against palmitic acid-induced inflammation, oxidative stress, and apoptosis through the JNK/NF-kB/NLRP3 pathway in cultured H9C2 cardiomyocytes. *J Cell Biochem* **120**:3651-3663.

Mitazaki S, Honma S, Suto M, Kato N, Hiraiwa K, Yoshida M and Abe S (2011) Interleukin-6 plays a protective role in development of cisplatin-induced acute renal failure through upregulation of anti-oxidative stress factors. *Life Sci* **88**:1142-1148.

Downloaded from molpharm.aspetjournals.org at ASPET Journals on April 19, 2024

Molecular Pharmacology Fast Forward. Published on January 26, 2023 as DOI: 10.1124/molpharm.122.000618
This article has not been copyedited and formatted. The final version may differ from this version.

Miyaji T, Kato A, Yasuda H, Fujigaki Y and Hishida A (2001) Role of the increase in p21 in cisplatin-induced acute renal failure in rats. *J Am Soc Nephrol* **12**:900-908.

Moradi H, Oveisi F, Khanifar E, Moreno-Sanz G, Vaziri ND and Piomelli D (2016) Increased Renal 2-Arachidonoylglycerol Level Is Associated with Improved Renal Function in a Mouse Model of Acute Kidney Injury. *Cannabis Cannabinoid Res* **1**:218-228.

Mowla SN, Perkins ND and Jat PS (2013) Friend or foe: emerging role of nuclear factor kappa-light-chain-enhancer of activated B cells in cell senescence. *Onco Targets Ther* **6**:1221-1229.

Mukhopadhyay P, Pan H, Rajesh M, Bátkai S, Patel V, Harvey-White J, Mukhopadhyay B, Haskó G, Gao B, Mackie K and Pacher P (2010) CB1 cannabinoid receptors promote oxidative/nitrosative stress, inflammation and cell death in a murine nephropathy model. *Br J Pharmacol* **160**:657-668.

Ozkok A and Edelstein CL (2014) Pathophysiology of cisplatin-induced acute kidney injury. *Biomed Res Int* **2014**:967826-967826.

Ozkok A, Ravichandran K, Wang Q, Ljubanovic D and Edelstein CL (2016) NF-κB transcriptional inhibition ameliorates cisplatin-induced acute kidney injury (AKI). *Toxicol Lett* **240**:105-113.

Parker LA, Limebeer CL, Rock EM, Litt DL, Kwiatkowska M and Piomelli D (2009) The FAAH inhibitor URB-597 interferes with cisplatin- and nicotine-induced vomiting in the Suncus murinus (house musk shrew). *Physiol Behav* **97**:121-124.

Peres LA and da Cunha AD, Jr. (2013) Acute nephrotoxicity of cisplatin: molecular mechanisms. *J Bras Nefrol* **35**:332-340.

Downloaded from molpharm.aspetjournals.org at ASPET Journals on April 19, 2024

Molecular Pharmacology Fast Forward. Published on January 26, 2023 as DOI: 10.1124/molpharm.122.000618
This article has not been copyedited and formatted. The final version may differ from this version.

Ritter JK, Li C, Xia M, Poklis JL, Lichtman AH, Abdullah RA, Dewey WL and Li PL (2012) Production and actions of the anandamide metabolite prostamide E2 in the renal medulla. *J Pharmacol Exp Ther* **342**:770-779.

Romero A, Dongil P, Valencia I, Vallejo S, Hipólito-Luengo Á S, Díaz-Araya G, Bartha JL, González-Arlanzón MM, Rivilla F, de la Cuesta F, Sánchez-Ferrer CF and Peiró C (2022) Pharmacological Blockade of NLRP3 Inflammasome/IL-1β-Positive Loop Mitigates Endothelial Cell Senescence and Dysfunction. *Aging Dis* **13**:284-297.

Rovillain E, Mansfield L, Caetano C, Alvarez-Fernandez M, Caballero OL, Medema RH, Hummerich H and Jat PS (2011) Activation of nuclear factor-kappa B signalling promotes cellular senescence. *Oncogene* **30**:2356-2366.

Ryan KM, Phillips AC and Vousden KH (2001) Regulation and function of the p53 tumor suppressor protein. *Curr Opin Cell Biol* **13**:332-327.

Salminen A, Kauppinen A and Kaarniranta K (2012) Emerging role of NF-κB signaling in the induction of senescence-associated secretory phenotype (SASP). *Cell Signal* **24**:835-845.

Sayd A, Antón M, Alén F, Caso JR, Pavón J, Leza JC, Rodríguez de Fonseca F, García-Bueno B and Orio L (2015) Systemic Administration of Oleoylethanolamide Protects from Neuroinflammation and Anhedonia Induced by LPS in Rats. *Int J Neuropsychopharmacol* **18**:pyu111.

Schlosser M, Löser, H. , Siegmund, S. , Montesinos-Rongen, M. , Bindila, L. , Lutz, B. , Barrett, D. , Sarmad, S. , Ortori, C. , Grau, V. , von Brandenstein, M. and Fries, J.

Downloaded from molpharm.aspetjournals.org at ASPET Journals on April 19, 2024

Molecular Pharmacology Fast Forward. Published on January 26, 2023 as DOI: 10.1124/molpharm.122.000618
This article has not been copyedited and formatted. The final version may differ from this version.

(2017) The Endocannabinoid, Anandamide, Induces Cannabinoid Receptor-Independent Cell Death in Renal Proximal Tubule Cells. *CellBio* **6**:33-55.

Sears SM and Siskind LJ (2021) Potential Therapeutic Targets for Cisplatin-Induced Kidney Injury: Lessons from Other Models of AKI and Fibrosis. *J Am Soc Nephrol* **32**:1559-1567.

Shamran H, Singh NP, Zumbrun EE, Murphy A, Taub DD, Mishra MK, Price RL, Chatterjee S, Nagarkatti M, Nagarkatti PS and Singh UP (2017) Fatty acid amide hydrolase (FAAH) blockade ameliorates experimental colitis by altering microRNA expression and suppressing inflammation. *Brain Behav Immun* **59**:10-20.

Sheekey E and Narita M (2021) p53 in senescence – it's a marathon not a sprint. *The FEBS Journal*:16425.

Shi L, Zhao Y, Fei C, Guo J, Jia Y, Wu D, Wu L and Chang C (2019) Cellular senescence induced by S100A9 in mesenchymal stromal cells through NLRP3 inflammasome activation. *Aging* **11**:9626-9642.

Uhelski ML, Khasabova IA and Simone DA (2015) Inhibition of anandamide hydrolysis attenuates nociceptor sensitization in a murine model of chemotherapy-induced peripheral neuropathy. *J Neurophysiol* **113**:1501-1510.

Uhlen M, Fagerberg L, Hallstrom BM, Lindskog C, Oksvold P, Mardinoglu A, Sivertsson A, Kampf C, Sjostedt E, Asplund A, Olsson I, Edlund K, Lundberg E, Navani S, Szigyarto CA, Odeberg J, Djureinovic D, Takanen JO, Hober S, Alm T, Edqvist PH, Berling H, Tegel H, Mulder J, Rockberg J, Nilsson P, Schwenk JM, Hamsten M, von Feilitzen K, Forsberg M, Persson L, Johansson F, Zwahlen M, von Heijne

Downloaded from molpharm.aspetjournals.org at ASPET Journals on April 19, 2024

Molecular Pharmacology Fast Forward. Published on January 26, 2023 as DOI: 10.1124/molpharm.122.000618
This article has not been copyedited and formatted. The final version may differ from this version.

G, Nielsen J and Ponten F (2015) Proteomics. Tissue-based map of the human proteome. *Science* **347**:1260419.

Winkler K, Ramer R, Dithmer S, Ivanov I, Merkord J and Hinz B (2016) Fatty acid amide hydrolase inhibitors confer anti-invasive and antimetastatic effects on lung cancer cells. *Oncotarget* **7**:15047-15064.

Wise LE, Harloe JP and Lichtman AH (2009) Fatty acid amide hydrolase (FAAH) knockout mice exhibit enhanced acquisition of an aversive, but not of an appetitive, Barnes maze task. *Neurobiol Learn Mem* **92**:597-601.

Xie D, Hu G, Chen C, Ahmadinejad F, Wang W, Li PL, Gewirtz DA and Li N (2022) Loss of sphingosine kinase 2 protects against cisplatin-induced kidney injury. *Am J Physiol Renal Physiol* **323**:F322-F334.

Xie D, Wang J, Hu G, Chen C, Yang H, Ritter JK, Qu Y and Li N (2021) Kidney-Targeted Delivery of Prolyl Hydroxylase Domain Protein 2 Small Interfering RNA with Nanoparticles Alleviated Renal Ischemia/Reperfusion Injury. *J Pharmacol Exp Ther* **378**:235-243.

Yan M and Ren H (2012) Involvement of Nuclear Factor Kappa B in High-Fat Diet-Related Pancreatic Fibrosis in Rats. *Gut Liver* **6**:381-387.

Yeh P, Yeh K, Chuang S, Song Y and Cheng A (2004) Suppression of MEK/ERK Signaling Pathway Enhances Cisplatin-induced NF-κB Activation by Protein Phosphatase 4-mediated NF-κB p65 Thr Dephosphorylation*. *J Biol Chem* **279**:26143-26148.

Yin Y, Zhou Z, Liu W, Chang Q, Sun G and Dai Y (2017) Vascular endothelial cells senescence is associated with NOD-like receptor family pyrin domain-containing

Downloaded from molpharm.aspetjournals.org at ASPET Journals on April 19, 2024

Molecular Pharmacology Fast Forward. Published on January 26, 2023 as DOI: 10.1124/molpharm.122.000618
This article has not been copyedited and formatted. The final version may differ from this version.

3 (NLRP3) inflammasome activation via reactive oxygen species (ROS)/thioredoxin-interacting protein (TXNIP) pathway. *Int J Biochem Cell Biol* **84**:22-34.

Yu LL, Yu HG, Yu JP, Luo HS, Xu XM and Li JH (2004) Nuclear factor-kappaB p65 (RelA) transcription factor is constitutively activated in human colorectal carcinoma tissue. *World J Gastroenterol* **10**:3255-3260.

Zhang D, Liu Y, Wei Q, Huo Y, Liu K, Liu F and Dong Z (2014) Tubular p53 Regulates Multiple Genes to Mediate AKI. *J Am Soc Nephrol* **25**:2278-2289.

Zhao K and Wen LB (2018) DMF attenuates cisplatin-induced kidney injury via activating Nrf2 signaling pathway and inhibiting NF-kB signaling pathway. *Eur Rev Med Pharmacol Sci* **22**:8924-8931.

Zhu S, Pabla N, Tang C, He L and Dong Z (2015) DNA damage response in cisplatin-induced nephrotoxicity. *Arch Toxicol* **89**:2197-2205.

Footnotes

This research was supported in part by the National Institutes of Health [Grant R01-HL145163, DK107991, DK102539] (to N.L.) and [Grant R01-CA239706, CA206028, CA260819] (to D.A.G.) Services and products in support of the research project were generated by the Virginia Commonwealth University Cancer Mouse Models Core Laboratory, supported, in part, with funding to the Massey Cancer Center from NIH-NCI Cancer Center Support Grant P30 CA016059. Mutant mice in support of the research project were generated by the Virginia Commonwealth University Cancer Transgenic/Knock-Out Mouse Shared Resource supported in part by funding from NIH

Downloaded from molpharm.aspetjournals.org at ASPET Journals on April 19, 2024

Molecular Pharmacology Fast Forward. Published on January 26, 2023 as DOI: 10.1124/molpharm.122.000618
This article has not been copyedited and formatted. The final version may differ from this version.

National Institute on Drug Abuse grant P30DA033934 (to L.H.A.). No author has an actual or perceived conflict of interest with the contents of this article.

Figure legends

Figure 1. Effects of cisplatin and *Faah* KO on renal function in mice. (A) Cisplatin (Cis) induced-concentrations of plasma creatinine and (B) blood urea nitrogen (BUN) in WT mice were reduced in *Faah*$^{-/-}$ mice (WT-Cis vs. *Faah*$^{-/-}$Cis: 3.0 ± 0.9 vs. 1.4 ± 0.9 mg/dL creatinine, $P < 0.05$; 156.6 ± 29.2 vs. 81.8 ± 27.4 mg/dL BUN, $P < 0.001$) at 72 h post exposure to cisplatin (30mg/kg). (C-D) Representative immunoblots and summarized data showing that *Faah*$^{-/-}$ mice had lower protein expression of kidney injury marker-1 (KIM-1) than WT-Cis mice (WT-Cis vs. *Faah*$^{-/-}$ Cis: 3.1 vs. 0.9 -fold change, $P < 0.0001$; no statistical difference between WT-saline and *Faah*$^{-/-}$Cis^{-}). All ratios of band intensities over GAPDH were obtained from each single sample and normalized to the mean value of the WT-saline group. *$P < 0.05$, ***$P < 0.001$, **** $P < 0.0001$ by one-way ANOVA with Bonferroni's post hoc test determining the differences between two groups (WT-saline vs. WT-Cis, WT-Cis vs. *Faah*$^{-/-}$ Cis). Data are shown as mean± SD (n = 5 mice/group). Cis: cisplatin.

Figure 2. Effects of cisplatin and *Faah* KO on cisplatin-induced body weight loss and renal pathology. (A) Change of the body weight (%) in WT and *Faah*$^{-/-}$ mice after cisplatin treatment (30mg/kg) (3.1 ± 1.8, -19.5 ± 1.5, -14.3 ± 1.1 % in WT-saline, WT-Cis and *Faah*$^{-/-}$ Cis, respectively; WT-saline vs. WT-Cis, $P < 0.0001$; WT-Cis vs. *Faah*$^{-/-}$

Downloaded from molpharm.aspetjournals.org at ASPET Journals on April 19, 2024

Molecular Pharmacology Fast Forward. Published on January 26, 2023 as DOI: 10.1124/molpharm.122.000618
This article has not been copyedited and formatted. The final version may differ from this version.

Cis, $P < 0.001$). (B) Representative kidney images of the fresh kidneys from WT and *Faah*$^{-/-}$ mice. Black bar = 50mm. (C) Representative photomicrographs and (D) semi-quantification of tubular injury scores of Periodic-Acid Schiff (PAS) staining as indicated by tubular atrophy, vacuolar degeneration, loss of brush border and cast formation in mice (WT-Cis vs. *Faah*$^{-/-}$ Cis: 3.6 ± 0.3 vs. 2.4 ± 0.2 points, $P < 0.0001$). (E) Percentage of positive area of cast formation in kidney tubules (WT-Cis vs. *Faah*$^{-/-}$ Cis: 13.18 ± 2.6 vs. 6.28 ± 1.4 %, $P < 0.0001$). Black bar = 100μm. ***$P < 0.001$, **** $P < 0.0001$ by one-way ANOVA with Bonferroni's post hoc test determining the differences between two groups (WT-saline vs. WT-Cis, WT-Cis vs. *Faah*$^{-/-}$ Cis). Data are shown as mean± SD.

Figure 3. Levels of endogenous endocannabinoids AEA, 2AG and arachidonic acid (AA) in mouse renal cortex. (A-B) Quantitative data of liquid chromatography/tandem mass spectrometry (LC-MS/MS) showing no difference in the levels of AEA, 2-AG and AA extracted from renal cortex of WT and *Faah*$^{-/-}$ mice. Values were normalized to tissue weight of mouse cortex. Data are presented as the relative fold change of AEA, 2-AG and AA in the experimental groups compared to the mean of the WT- saline group. ** $P < 0.01$, ns: not significant by one-way ANOVA with Bonferroni's post hoc test determining the differences between two groups (WT-saline vs. WT-Cis, WT-Cis vs. *Faah*$^{-/-}$ Cis). Data are shown as mean± SD.

Figure 4. Levels of two fatty acid ethanolamides, PEA and OEA in mouse renal cortex. (A-B) Representative liquid chromatography/tandem mass spectrometry (LC-MS/MS) chromatograms of PEA and OEA extracted from mouse renal cortex. PEA/OEA

Downloaded from molpharm.aspetjournals.org at ASPET Journals on April 19, 2024

Molecular Pharmacology Fast Forward. Published on January 26, 2023 as DOI: 10.1124/molpharm.122.000618
This article has not been copyedited and formatted. The final version may differ from this version.

(blue) & PEA-d_8/OEA-d_8 (red, internal standard) from renal cortex extracts. Y-axis (intensity of PEA or OEA, CPS, count/s per second) and X-axis (retention time of PEA or OEA). (C-D) Quantitative data of LC-MS/MS showing levels of PEA (C) and OEA (D) were higher in *Faah*$^{-/-}$ Cis than those in WT-Cis mice (WT-Cis vs. *Faah*$^{-/-}$ Cis: 0.6 vs. 1 - fold change in PEA levels, $P = 0.0109$; 0.9 vs. 2.9-fold change in OEA levels, $P < 0.0001$). Values were normalized to tissue weight of mouse cortex**.** Data are presented as the relative fold change of PEA and OEA in the experimental groups compared to the mean of the WT- saline group. *$P < 0.05$, **** $P < 0.0001$, ns: not significant by one-way ANOVA Bonferroni's post hoc test determining the differences between two groups (WT-saline vs. WT-Cis, WT-Cis vs. *Faah*$^{-/-}$ Cis). Data are shown as mean± SD.

Figure 5. Effect of *Faah* KO on cisplatin-induced nuclear translocation of NF-κB/p65 in mouse kidneys. (A) Representative immunohistochemical staining showing the nuclear translocation of nuclear NF-κB/p65 (red arrows) in mouse kidney tissue. At least 10 fields for each sample were assessed for all results. Black bar = 50μm. (B) The average number of cells with NF-κB/p65 positive stained nuclei (brown) in mouse kidneys were calculated per high power field (x 400). Results showed that *Faah*$^{-/-}$ cisplatin mice exhibited lower cisplatin-induced nuclear expression of NF-κB/p65 than those in WT-Cis mice (WT-Cis vs. *Faah*$^{-/-}$ Cis: 51 vs. 18 positive cells/power field, $P = 0.0021$). **$P < 0.01$, *** $P < 0.001$ by one-way ANOVA Bonferroni's post hoc test determining the differences between two groups (WT-saline vs. WT-Cis, WT-Cis vs. *Faah*$^{-/-}$ Cis). Data are shown as mean± SD.

Downloaded from molpharm.aspetjournals.org at ASPET Journals on April 19, 2024

Molecular Pharmacology Fast Forward. Published on January 26, 2023 as DOI: 10.1124/molpharm.122.000618
This article has not been copyedited and formatted. The final version may differ from this version.

Figure 6. Effect of *Faah* KO on inflammatory factors in renal cortex. (A-D) Representative immunoblots and quantitative data showing the levels of inflammasome-mediated caspase-1 and IL-1β activation. Cisplatin-induced protein expression of cleaved caspase-1 (A, B) and mature IL-1β (C, D) in WT mice were decreased in *Faah*$^{-/-}$ Cis mice (2.5 vs. 0.99 -fold change in cleaved caspase-1, $P < 0.0001$; 6.9 vs. 2.5-fold change in IL-1β, $P = 0.0067$). All ratios of band intensities over loading control (GAPDH) were obtained from each single sample and normalized to the mean value of the WT-saline group. (E) Representative immunohistochemical staining showing the expression of (F) CD68 (9.5 vs. 4.2-fold, WT-Cis vs. *Faah*$^{-/-}$ Cis, $P = 0.0073$) and (F) CD43 (13.3 vs. 6.7 -fold change, WT-Cis vs. *Faah*$^{-/-}$ Cis, $P = 0.001$). Black bar = 100mm. ** $P < 0.01$, ***$P < 0.001$, **** $P < 0.0001$ by one-way ANOVA Bonferroni's post hoc test determining the differences between two groups (WT-saline vs. WT-Cis, WT-Cis vs. *Faah*$^{-/-}$ Cis). Data are shown as mean± SD.

Figure 7. Effect of *Faah* KO on the expression of DNA damage markers in mouse renal cortex. (A-D) Representative immunoblots and quantitative data showing that the increased levels of DNA damage markers p53 (A, B) and p21 (C, D) in WT-Cis mice were reduced in *Faah*$^{-/-}$ mice (6.4 vs. 2.4 -fold change in p53, $P = 0.049$; 22 vs. 5.1 -fold change in p21, $P < 0.0001$). All ratios of band intensities over loading control (GAPDH) were obtained from each single sample and normalized to the mean value of the WT-saline group. *$P < 0.05$, **** $P < 0.0001$ by one-way ANOVA Bonferroni's post hoc test determining the differences between two groups (WT-saline vs. WT-Cis, WT-Cis vs. *Faah*$^{-/-}$ Cis). Data are shown as mean± SD.

Downloaded from molpharm.aspetjournals.org at ASPET Journals on April 19, 2024

Molecular Pharmacology Fast Forward. Published on January 26, 2023 as DOI: 10.1124/molpharm.122.000618
This article has not been copyedited and formatted. The final version may differ from this version.

Figure 8. Effect of the FAAH inhibitor on cisplatin-induced toxicity in human head and neck squamous cell carcinoma cell lines, HN30 and HN12. (A) MTS assay showing that there was no difference between the cell viability of HN30 (p53 wild-type) and (B) HN12 (p53 mutant) following difference doses of cisplatin (0 μM to 20 μM) with or without the FAAH inhibitor (PF), PF-04457845, (1 μM and 2 μM) treatment on Day 3 and Day 6. (C) Clonogenic survival assay showing no difference in toxicity (colony formation) between the cisplatin alone group and Combo (5 μM Cis + 1 μM PF) when HN30 and HN12 cells were subjected to cisplatin in the absence and presence of PF-04457845. All graphs are presented as mean ± SD and obtained from as at least three independent experiments (biological replicates), all of which were conducted in triplicates or duplicates (technical replicates). D: day. PF: PF-04457845. Cis: cisplatin. ns: not significant by one-way ANOVA with Bonferroni's post hoc test determining the differences between two groups.

Figure 9. Proposed mechanism of FAAH inactivation in preventing cisplatin-induced DNA damage response, inflammation, and nephrotoxicity. FAAH inhibition is proposed to reduce the activation of NF-κB/p65, decrease the expression of DNA damage markers p53, p21, cleaved caspase-1 and IL-1β and infiltration of macrophages and leukocytes. The consequent inhibition of the positive loop of inflammation and DNA damage response by FAAH inactivation leads to the attenuation of cisplatin-induced nephrotoxicity.

Downloaded from molpharm.aspetjournals.org at ASPET Journals on April 19, 2024

Molecular Pharmacology Fast Forward. Published on January 26, 2023 as DOI: 10.1124/molpharm.122.000618
This article has not been copyedited and formatted. The final version may differ from this version.

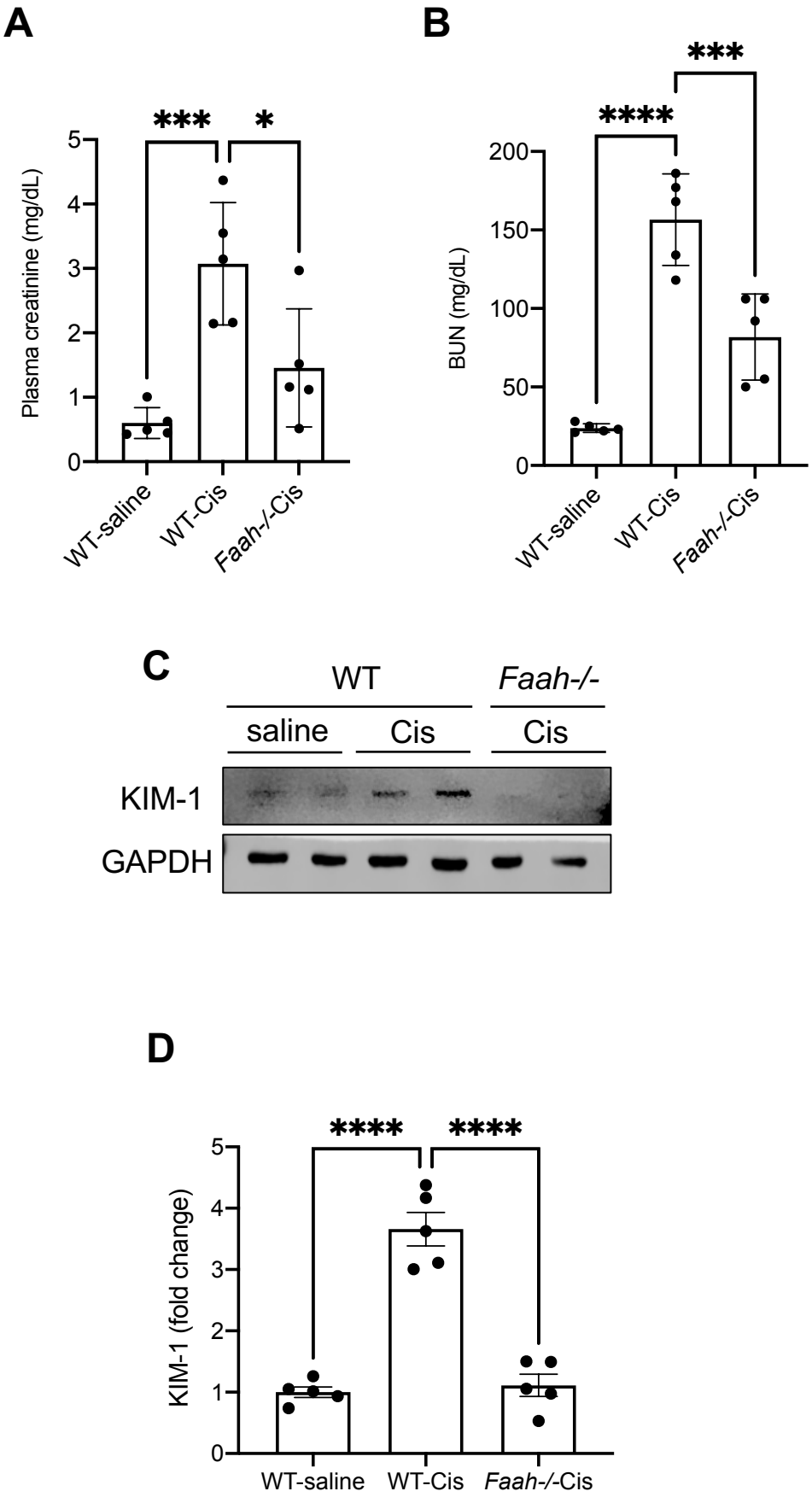

Figure 1

Downloaded from molpharm.aspetjournals.org at ASPET Journals on April 19, 2024

Molecular Pharmacology Fast Forward. Published on January 26, 2023 as DOI: 10.1124/molpharm.122.000618
This article has not been copyedited and formatted. The final version may differ from this version.

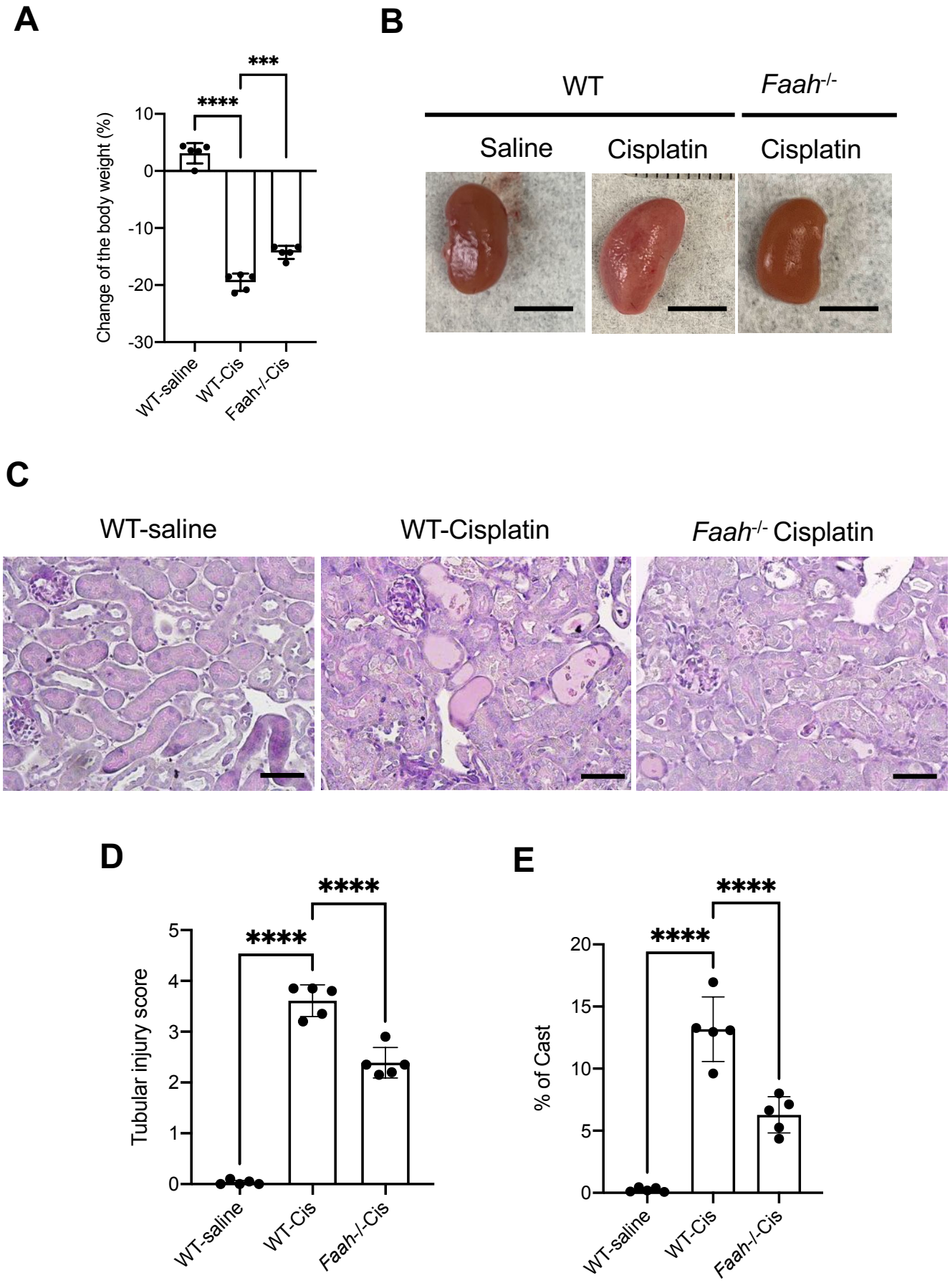

Figure 2

Downloaded from molpharm.aspetjournals.org at ASPET Journals on April 19, 2024

Molecular Pharmacology Fast Forward. Published on January 26, 2023 as DOI: 10.1124/molpharm.122.000618
This article has not been copyedited and formatted. The final version may differ from this version.

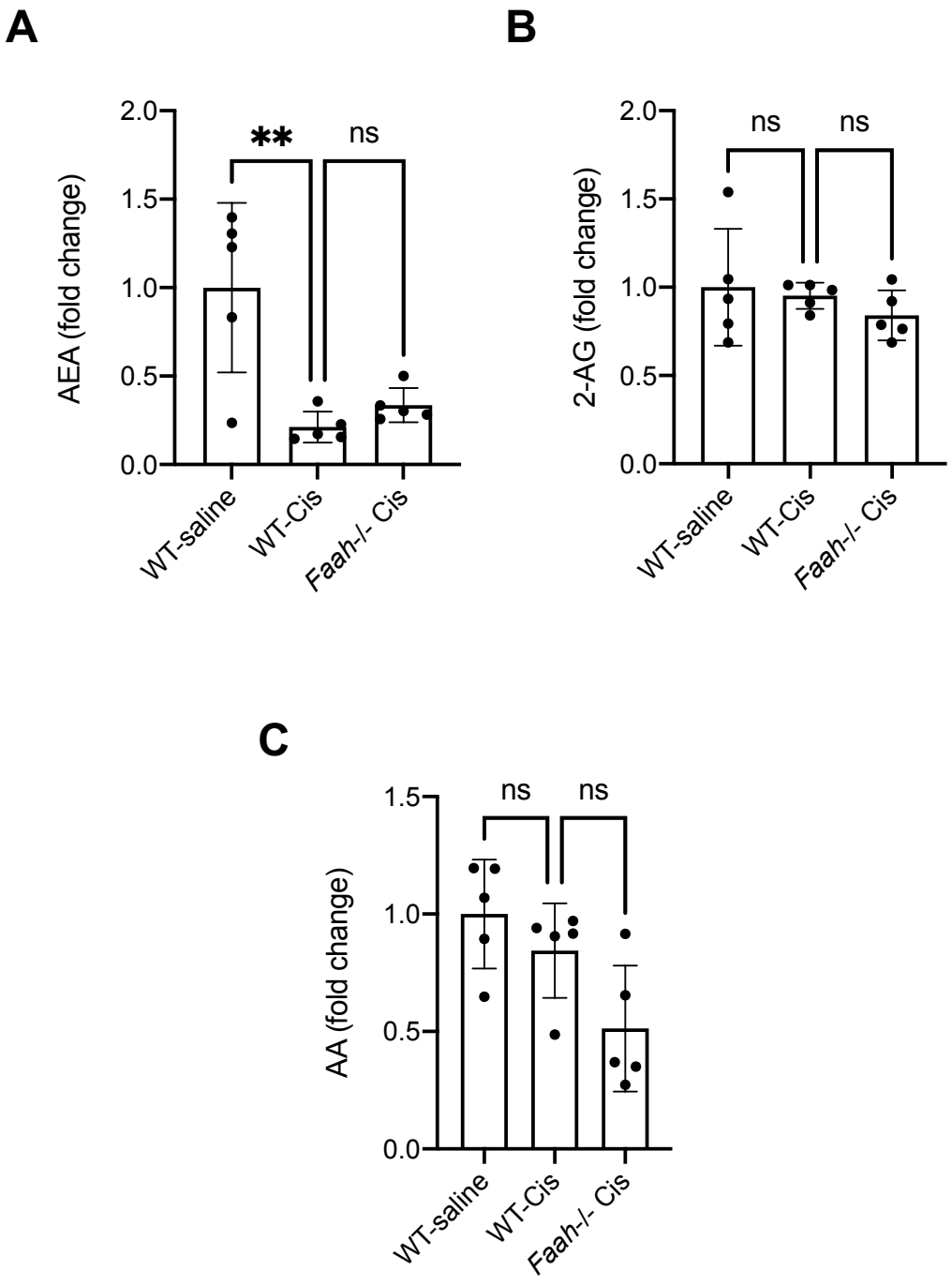

Figure 3

Downloaded from molpharm.aspetjournals.org at ASPET Journals on April 19, 2024

Molecular Pharmacology Fast Forward. Published on January 26, 2023 as DOI: 10.1124/molpharm.122.000618
This article has not been copyedited and formatted. The final version may differ from this version.

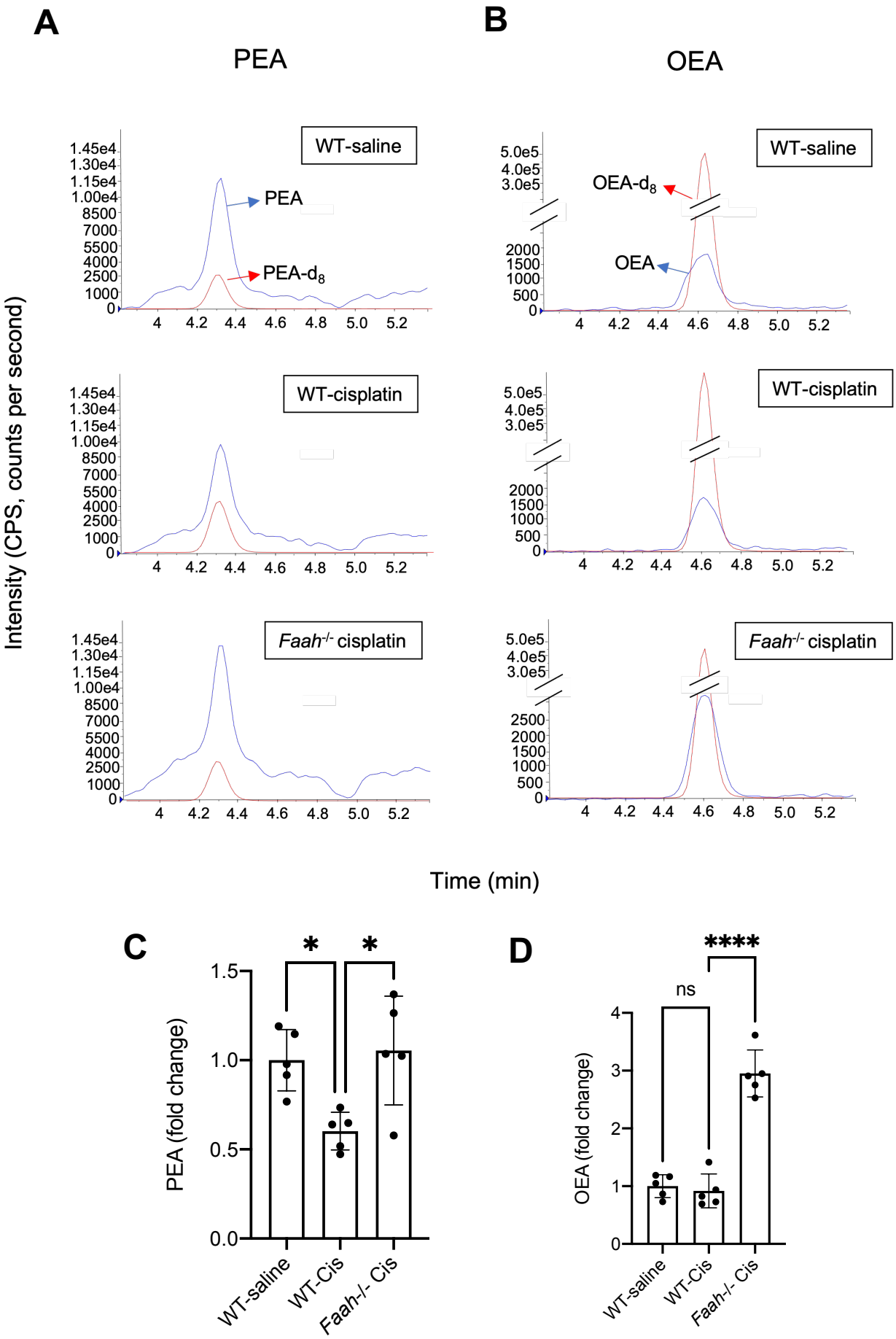

Figure 4

Downloaded from molpharm.aspetjournals.org at ASPET Journals on April 19, 2024

Molecular Pharmacology Fast Forward. Published on January 26, 2023 as DOI: 10.1124/molpharm.122.000618
This article has not been copyedited and formatted. The final version may differ from this version.

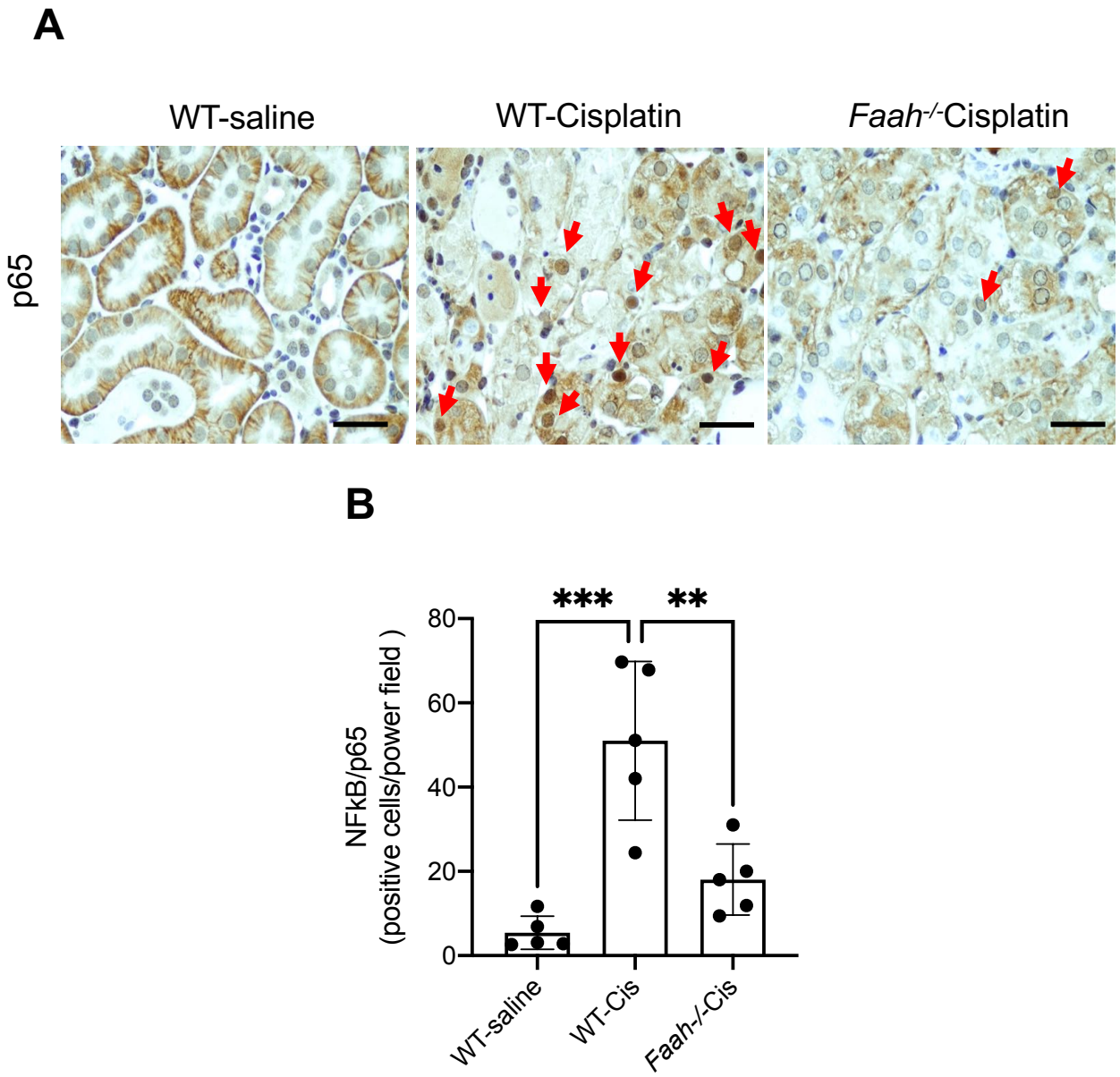

Figure 5

Downloaded from molpharm.aspetjournals.org at ASPET Journals on April 19, 2024

Molecular Pharmacology Fast Forward. Published on January 26, 2023 as DOI: 10.1124/molpharm.122.000618
This article has not been copyedited and formatted. The final version may differ from this version.

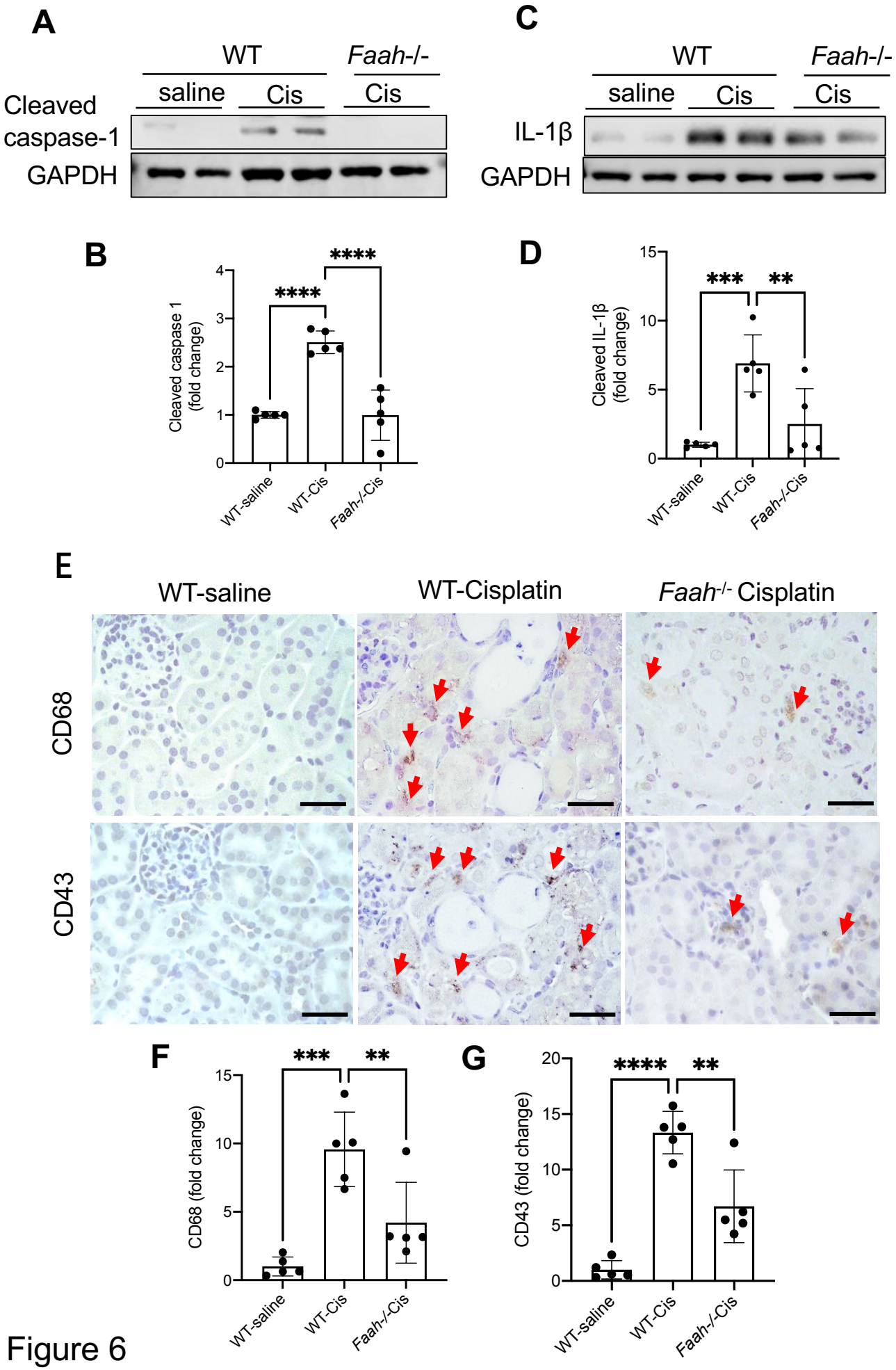

Figure 6

Downloaded from molpharm.aspetjournals.org at ASPET Journals on April 19, 2024

Molecular Pharmacology Fast Forward. Published on January 26, 2023 as DOI: 10.1124/molpharm.122.000618
This article has not been copyedited and formatted. The final version may differ from this version.

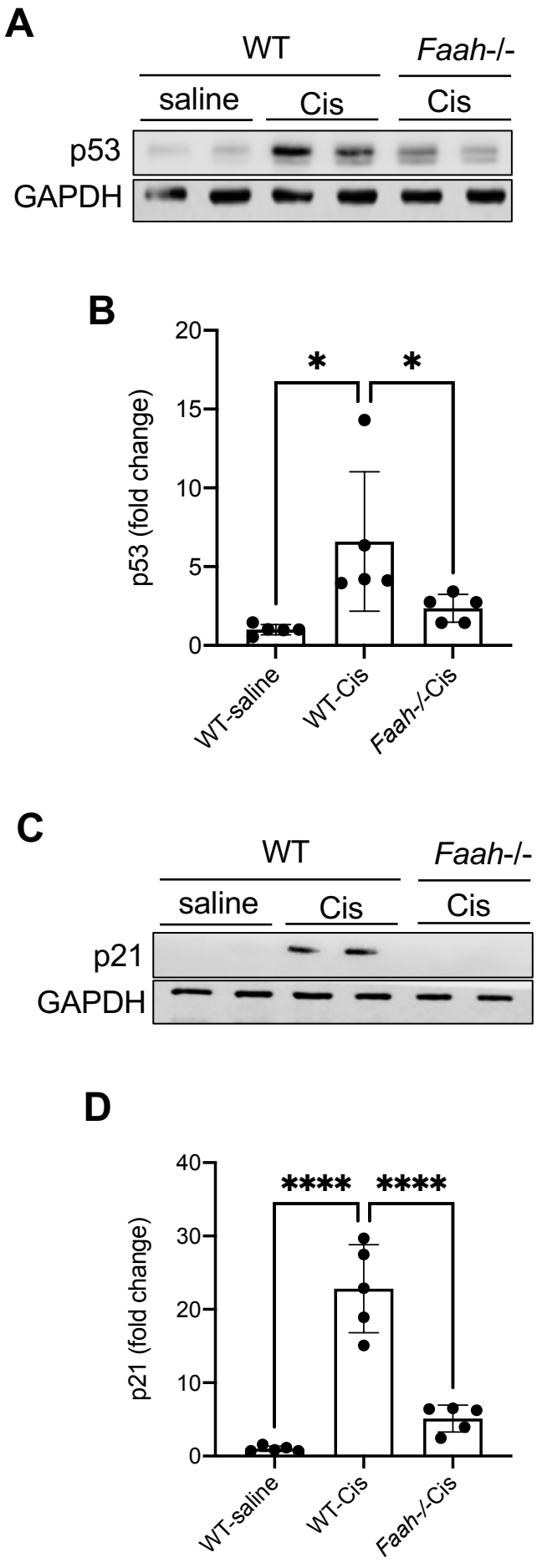

Figure 7

Downloaded from molpharm.aspetjournals.org at ASPET Journals on April 19, 2024

Molecular Pharmacology Fast Forward. Published on January 26, 2023 as DOI: 10.1124/molpharm.122.000618
This article has not been copyedited and formatted. The final version may differ from this version.

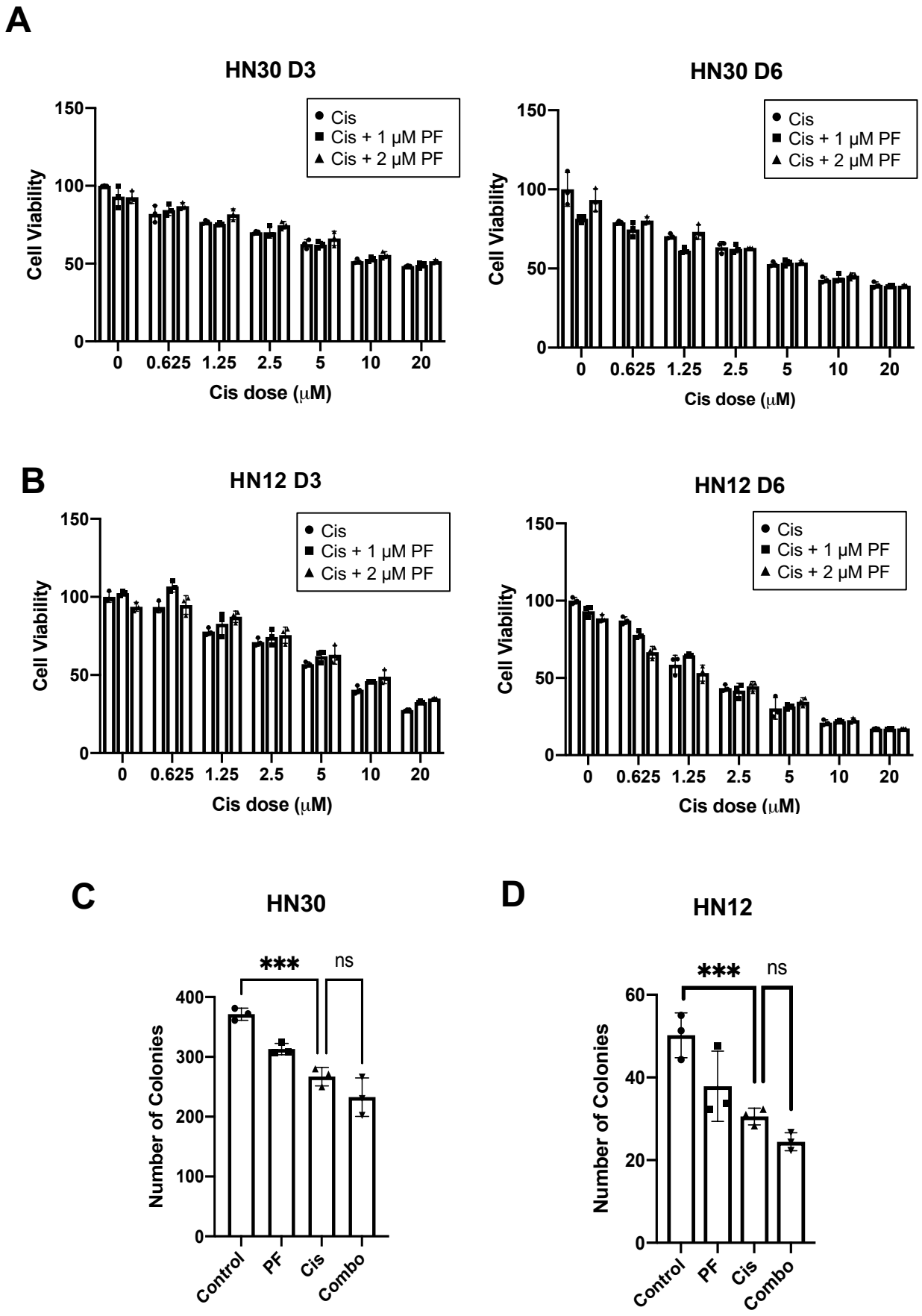

Figure 8

Downloaded from molpharm.aspetjournals.org at ASPET Journals on April 19, 2024

Molecular Pharmacology Fast Forward. Published on January 26, 2023 as DOI: 10.1124/molpharm.122.000618
This article has not been copyedited and formatted. The final version may differ from this version.

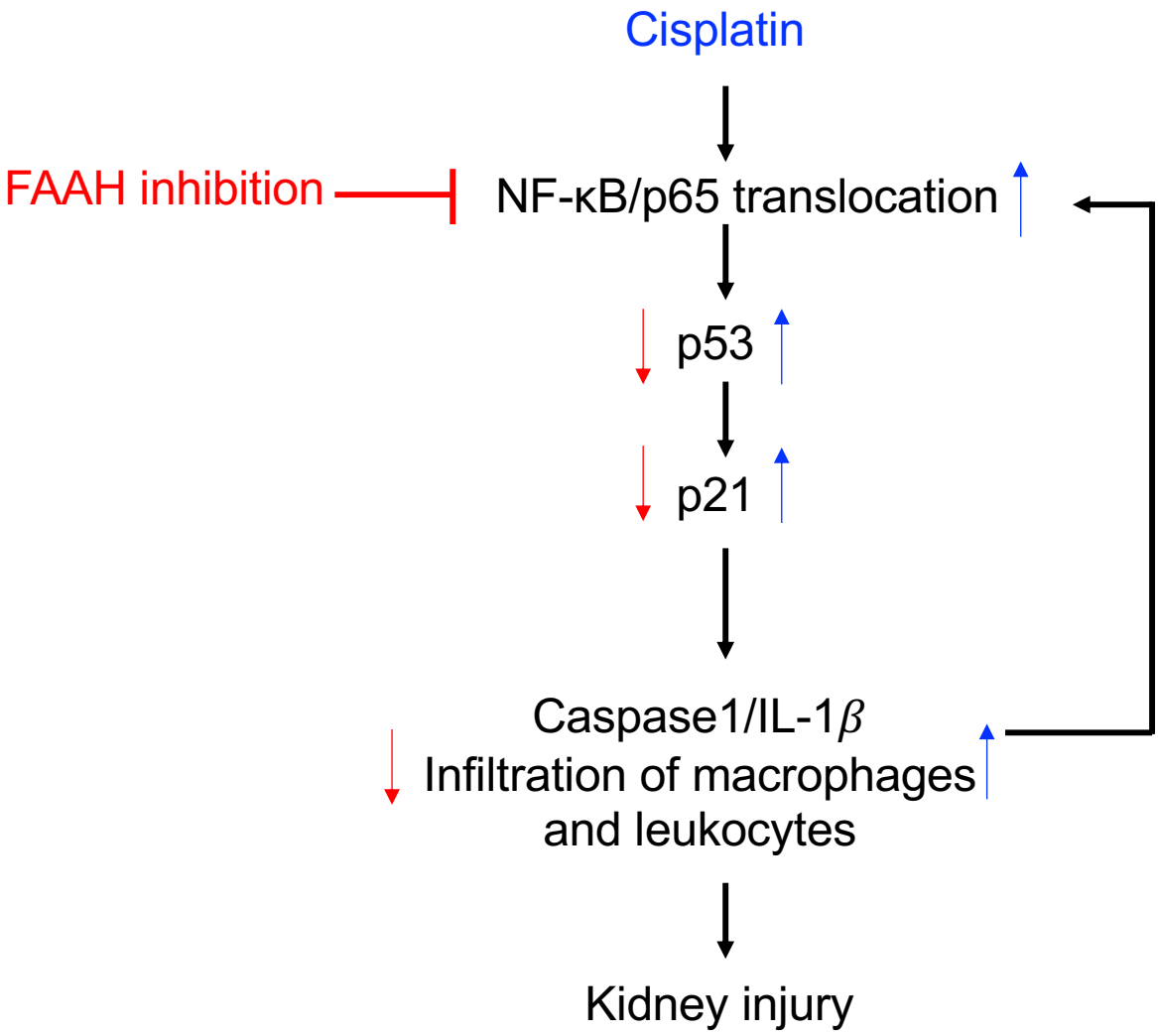

Figure 9

Downloaded from molpharm.aspetjournals.org at ASPET Journals on April 19, 2024